iScience

CellPress
OPEN ACCESS

Article

# MMP9 drives ferroptosis by regulating GPX4 and iron signaling

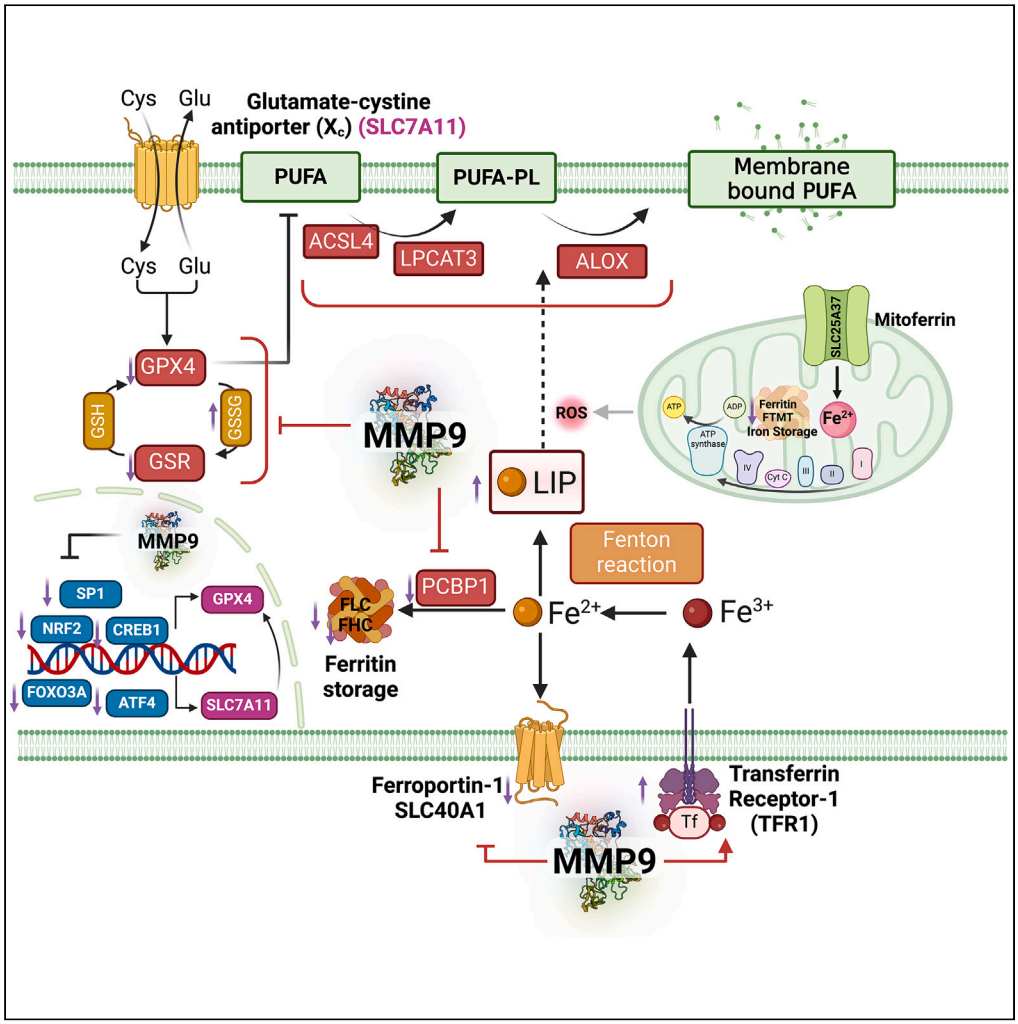


Flobater I. Gawargi, Paras K. Mishra

paraskumar.mishra@unmc.edu

## Highlights

MMP9 expression varies in the cytoplasm, mitochondria, and nucleus

MMP9 disrupts cellular redox balance by regulating GPX4 transcription and activity

MMP9 promotes iron accumulation by regulating import, storage, and export

MMP9 interacts with at least 83 subcellular proteins to regulate ferroptosis

Gawargi & Mishra, iScience 27, 110622
September 20, 2024 
https://doi.org/10.1016/j.isci.2024.110622

iScience

CellPress
OPEN ACCESS

Article

# MMP9 drives ferroptosis by regulating GPX4 and iron signaling

Flobater I. Gawargi[1] and Paras K. Mishra[1,2,*]

## SUMMARY

**Ferroptosis, defined by the suppression of glutathione peroxidase-4 (GPX4) and iron overload, is a distinctive form of regulated cell death. Our in-depth research identifies matrix metalloproteinase-9 (MMP9) as a critical modulator of ferroptosis through its influence on GPX4 and iron homeostasis. Employing an innovative MMP9 construct without collagenase activity, we reveal that active MMP9 interacts with GPX4 and glutathione reductase, reducing GPX4 expression and activity. Furthermore, MMP9 suppresses key transcription factors (SP1, CREB1, NRF2, FOXO3, and ATF4), alongside GPX1 and ferroptosis suppressor protein-1 (FSP1), thereby disrupting the cellular redox balance. MMP9 regulates iron metabolism by modulating iron import, storage, and export via a network of protein interactions. LC-MS/MS has identified 83 proteins that interact with MMP9 at subcellular levels, implicating them in ferroptosis regulation. Integrated pathway analysis (IPA) highlights MMP9's extensive influence on ferroptosis pathways, underscoring its potential as a therapeutic target in conditions with altered redox homeostasis and iron metabolism.**

## INTRODUCTION

Ferroptosis is an iron-driven process of cell death, distinctively marked by lipid peroxidation, and increasingly recognized for its relevance to a myriad of disease processes.[1,2] It plays a significant role in the development of human heart failure.[3] The regulation of ferroptosis involves a complex interplay of molecular pathways that are still being unraveled.[4] At the core of this regulation is glutathione peroxidase-4 (GPX4), a vital enzyme that acts as a gatekeeper against oxidative damage by reducing lipid hydroperoxides.[4,5] Its activity is supported by a tightly regulated glutathione cycle, which depends on the import of cysteine through system xc− and is sustained by the action of glutathione reductase (GSR).[6,7] The expression and activity of GPX4 are further fine-tuned at the transcriptional level by an array of nuclear factors, including specificity protein 1 (SP1), cAMP response element-binding protein (CREB), forkhead box O3 (FOXO3), activating transcription factor 4 (ATF4), and nuclear factor erythroid 2–related factor 2 (NRF2), which together modulate its transcriptional response to oxidative stress.[7–12] Complementarily, glutathione peroxidase-1 (GPX1), another selenoenzyme, contributes to the cellular antioxidant defense by reducing hydrogen peroxide and soluble lipid hydroperoxides.[13] In addition to the GPX4-centric mechanisms, the ferroptosis suppressor protein-1 (FSP1) has been identified as an alternative, GPX4-independent defender, contributing to the reduction of lipid peroxides and thus serving as another layer of protection against ferroptosis.[14] Despite these advances, a comprehensive understanding of how these GPX4-dependent and independent pathways are integrated and regulated to control ferroptosis remains an elusive yet critical aspect of this cell death modality.

Ferrous iron ($Fe^{2+}$) catalyzes ferroptosis by transforming lipid hydroperoxides into peroxides, leading to cellular membrane damage and cell death.[4] Heme metabolism, driven by heme oxygenase-1 (HMOX1), and iron uptake via the transferrin receptor (TFR) both escalate $Fe^{2+}$ levels, thereby promoting ferroptosis.[4,15] On the other hand, the export of iron via ferroportin-1 (FPN-1) and its sequestration into ferritin, which consists of heavy and light chains, serve to reduce $Fe^{2+}$ levels.[16,17] Specifically, the downregulation of ferritin light chain and the activity of poly(rC)-binding protein 1 (PCBP1), which facilitates iron storage, enhance ferroptosis.[18,19] NRF2 opposes this process by both reducing $Fe^{2+}$ and upregulating GPX4.[12,20,21] Additionally, mitochondrial sequestration of iron via mitoferrin-1 (MFRN1) and storage in mitochondrial ferritin (FTMT) also diminishes cytosolic $Fe^{2+}$ levels, impeding ferroptosis.[22,23] Nonetheless, the intricate regulation of iron homeostasis, particularly the upregulation mechanisms of $Fe^{2+}$ in ferroptosis, is not fully understood.

Matrix metalloproteinase-9 (MMP9), a collagenase known for its role in disease pathogenesis, stands out as a promising target for clinical therapies.[24] Although its activation by phorbol 12-myristate 13-acetate (PMA) and extracellular functions are well characterized, its intracellular roles, especially in non-collagenase activities, are not fully understood.[25–28] Emerging studies point to MMP9's influence on epigenetic control, autophagy, and cell death through promoting oxidative and inflammatory responses.[29,30] Sparse research into its non-collagenase functions reveals effects on key signaling pathways including ERK and PTEN and potential modulation of SOD3.[31,32] Despite the link between

[1]Department of Cellular and Integrative Physiology, University of Nebraska Medical Center, Omaha, NE, USA
[2]Lead contact
*Correspondence: paraskumar.mishra@unmc.edu
https://doi.org/10.1016/j.isci.2024.110622

ferroptosis and oxidative stress, MMP9's specific role in this cell death process is yet to be elucidated. In this study, we examined MMP9's subcellular dynamics and elucidated MMP9's pivotal role in the ferroptosis pathway, revealing how it orchestrates a complex network of protein interactions that regulate both GPX4 and $Fe^{2+}$, thereby shedding light on its potential as a therapeutic target in the modulation of this iron-dependent cell death mechanism.

## RESULTS

### Subcellular localization of MMP9 and effect of MMP9 expression versus collagenase activity on cell death

As MMP9 is a secretory protein, we evaluated whether MMP9 is present inside the cell by determining its subcellular localization. MMP9 is latent in the normal cells and is mostly upregulated and activated in pathological conditions.[33] However, pathological condition instigates multiple cellular signaling pathways that creates difficulty in delineating MMP9-induced specific cellular signaling pathways. Therefore, we used a normal cell model instead of a diseased one to investigate MMP9-induced cellular signaling by overexpressing and activating MMP9. To eliminate the possibility that altered subcellular localization of MMP9 might result from modifications in its secretory signals, we employed a full-length MMP9 construct (Figure S1). A plasmid-based transfection method was utilized to achieve overexpression of the full-length MMP9 in our cellular models as previously reported.[34] To avoid transfection-efficiency-related issues, we used transfection-efficient HEK293 cells.[35] We overexpressed MMP9 using a plasmid vector (referred to as MMP9), followed by stimulation with phorbol 12-myristate 13-acetate (PMA) to activate the overexpressed enzyme (denoted as MMP9+PMA). Cells that were neither transfected nor treated served as the control group (CT).

To determine the intracellular/subcellular localization of MMP9, we performed cell fractionation and isolated cytosolic, mitochondrial, and nuclear fraction. Immunoblot analysis of subcellular fractions revealed the presence of MMP9 in the cytoplasm, mitochondria, and nucleus, as evidenced by colocalization with the cytosolic marker GAPDH, the mitochondrial marker ATP5A, and the nuclear marker histone H3, respectively (Figure 1A). The expression of GAPDH varies in the cell fractions, with high expression in the cytosolic fraction, low expression in mitochondrial fraction, and no expression in the nuclear fraction (Figures S2A–S2C). MMP9 expression was elevated in the cytosolic fractions of both MMP9 and MMP9+PMA groups (Figure 1A). Remarkably, PMA treatment resulted in an increase of MMP9 levels in both the mitochondrial and nuclear fractions, with the nuclear fraction of the MMP9+PMA group displaying a 3-fold enhancement in MMP9 levels compared to the MMP9 group (Figure 1A). These data not only confirm the subcellular distribution of MMP9 but also indicate that PMA treatment results in a differential enhancement of MMP9 across various cellular compartments.

To distinguish between the expression and enzymatic activity effects of MMP9, we engineered a mutant form of MMP9 with a mutation in the active site. This mutation preserved the overall structure of the protein, analogous to the wild-type MMP9, as confirmed by structural analyses (Figures S3A and S3B; Videos S1). The enzymatic activity of the mutant MMP9 was assessed using in-gel gelatin zymography, which revealed a complete loss of collagenase activity, aligning it with the basal activity levels of control (CT) cells (Figure 1B). In contrast, MMP9 activity was substantially elevated in the MMP9+PMA group, serving as a positive control, thus confirming the increase in MMP9 activity upon overexpression (Figure 1B). Unexpectedly, treatment with a commercial MMP9 inhibitor (iMMP9) did not attenuate the activity in MMP9 group (Figure 1B), suggesting potential transient inhibition by iMMP9. Consequently, the iMMP9 treatment group was omitted from subsequent experiments.

In the context of ferroptosis, our study probed the role of MMP9 in initiating this process. To this end, we quantified cytotoxicity—a precursor to cell death—in cells overexpressing active (MMP9 group) and a catalytically inactive mutant form of MMP9 (MUT group). Although the MUT cells exhibited heightened MMP9 expression levels, their enzymatic activity was absent, as evidenced by Figures 1B and 1C. We included cells transfected with a scrambled plasmid (SC group) and non-transfected cells (NC group) as controls, which, as illustrated in Figure 1D, showed similar cytotoxicity profiles, thereby discounting the transfection procedure as a source of cytotoxic stress. Intriguingly, the MMP9 group displayed increased cytotoxicity, whereas the MUT group showed a reduction when compared against the SC group (Figure 1D). This disparity underscores the notion that MMP9's enzymatic activity is a key driver of cytotoxicity. Furthermore, our findings reveal a nuanced interplay where MMP9's expression and its enzymatic function independently modulate cellular cytotoxicity, collectively influencing the progression to cell death.

### MMP9 regulates GPX4 expression and activity

To determine the specific role of MMP9 in ferroptosis, we determined GPX4 expression and activity. GPX4 is a major antioxidant for lipid hydroperoxides, and reduced GPX4 is a key marker of ferroptosis.[4,5] We performed immunoblotting of GPX4 on proteins obtained from the three experimental groups: control (CT), MMP9, and mutant (MUT). Overexpression of MMP9 downregulated GPX4, whereas the lack of MMP9 activity prevented MMP9-mediated downregulation of GPX4 (Figure 2A). This result showed that MMP9 negatively regulates GPX4, and the activity of MMP9 is essential for GPX4 inhibition.

To explore how MMP9 downregulates GPX4, we assessed the protein-protein interaction between MMP9 and GPX4 using coimmunoprecipitation (co-IP). Our observations revealed that MMP9 immunoprecipitated proteins exhibit GPX4 expression in both MMP9 and MUT groups (Figure 2B). This finding indicates that MMP9 binds to GPX4, leading to a reduction in its levels. Given the presence of GPX4 in both cytosolic and mitochondrial fractions, it suggests that MMP9 can interact with GPX4 in both cell compartments (Figures 1A, S4A, and S4B). The co-IP results confirm MMP9's binding to GPX4 (Figure 2B), demonstrating that the activity of MMP9 is essential for the downregulation of GPX4 (Figure 1A).

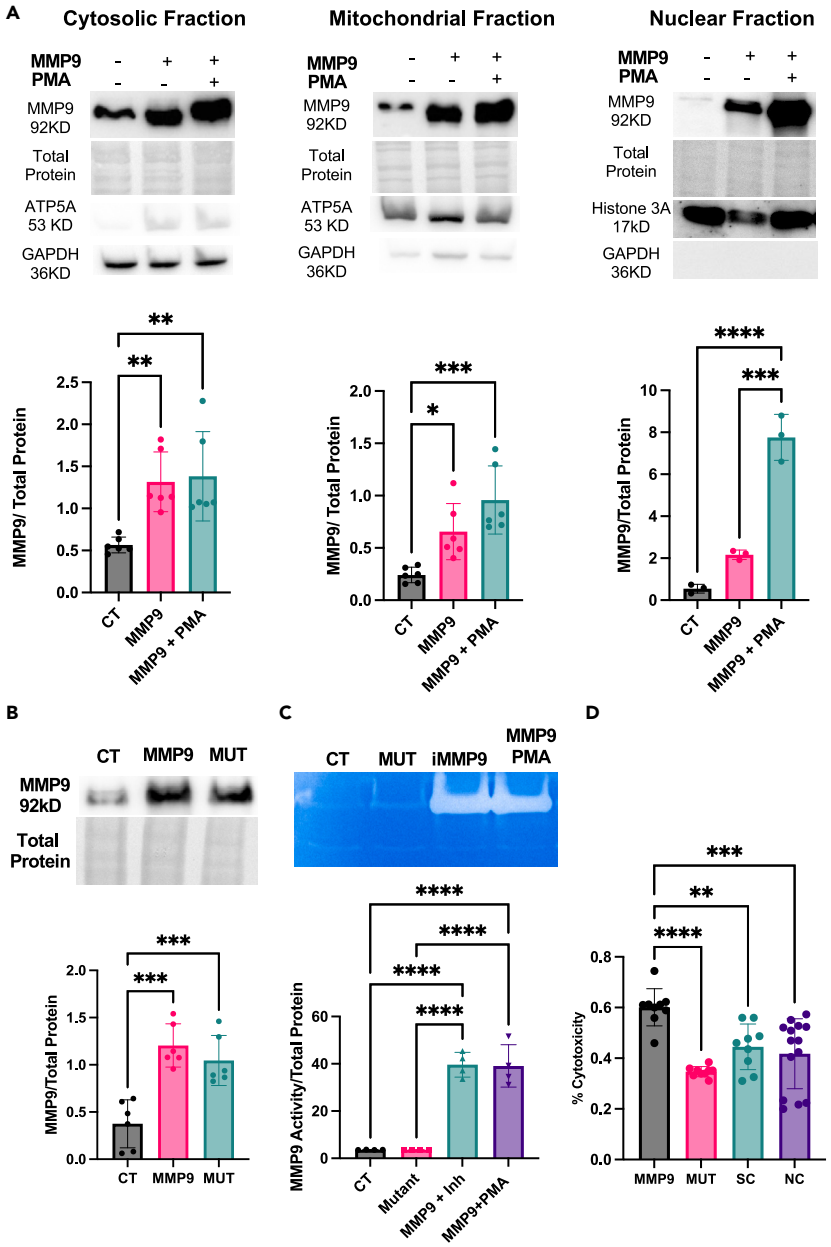


**Figure 1. Validation and characterization of MMP9 expression and activity in HEK293 cells**

(A) Subcellular distribution of MMP9: immunoblot analysis demonstrates MMP9's presence in cytosolic, mitochondrial, and nuclear fractions, indicating its ubiquitous distribution within the cell.

(B) Immunoblot analysis demonstrating the cellular expression levels of MMP9. There is a marked increase in MMP9 expression in cells overexpressing the active form of MMP9 and the collagenase activity mutant (MUT) MMP9, compared to control cells.

(C) Functional assessment of MMP9 enzymatic activity: in-gel gelatin zymography reveals the absence of proteolytic activity in the control (CT) and mutant MMP9, whereas the presence of white bands in MMP9 overexpressing and PMA-treated (MMP9+PMA) cells confirms an increase in MMP9 activity, which is not inhibited by the MMP9 inhibitor treatment (iMMP9) in MMP9-overexpressing cells. One-way ANOVA followed by Tukey's post hoc test was performed for statistical analysis from A to C, with each point representing an individual sample (n = 3–6).

(D) MMP9's impact on cell death: quantitative analysis of cytotoxicity by lactate dehydrogenase (LDH) assay reveals that increased MMP9 activity augments, whereas the lack of MMP9 activity (MUT) diminishes cytotoxicity. Data are presented as mean +/- standard deviation. Two-way ANOVA followed by Tukey's post hoc test was used for statistical analysis, with each point representing an individual sample (n = 9–14). $^{**}p < 0.01$; $^{***}p < 0.001$; $^{****}p < 0.0001$.

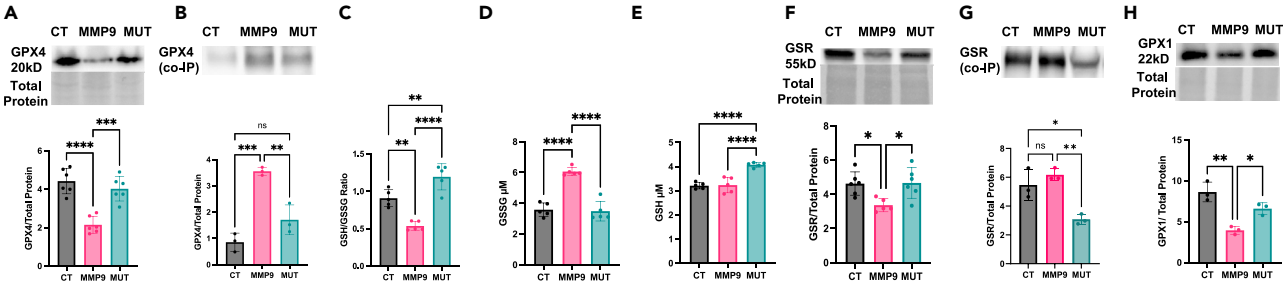


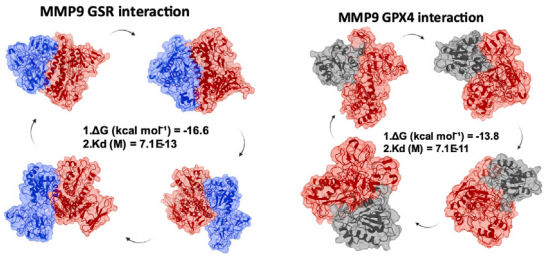


K

ClusPro model scores:

| Complex | Cluster | Members (docked conformations) | Representative | Weighted score KJ/mol |
|---|---|---|---|---|
| MMP9-GSR complex | 8 | 53 | Center | -1172.1 |
| | | | Lowest energy | -1399.4 |
| MMP9-GPX4 Complex | 2.2 | 66 | Center | -806.5 |
| | | | Lowest energy | -912.7 |

L PRODIGY ANALYSIS

| Protein-protein complex | ΔG (kcal mol-1) | Kd(M) at 25 ℃ | ICs charged-charged | ICs charged-polar | ICs charged-apolar | ICs polar-polar | ICs polar-apolar | ICs apolar-apolar | NIS charged | NIS apolar |
|---|---|---|---|---|---|---|---|---|---|---|
| MMP9-GSR Complex | -16.6 | 7.10E-13 | 20 | 16 | 51 | 5 | 28 | 37 | 27.17 | 42.77 |
| MMP9-GPX4 Complex | -13.8 | 7.10E-11 | 21 | 22 | 50 | 4 | 16 | 21 | 28.61 | 42.79 |

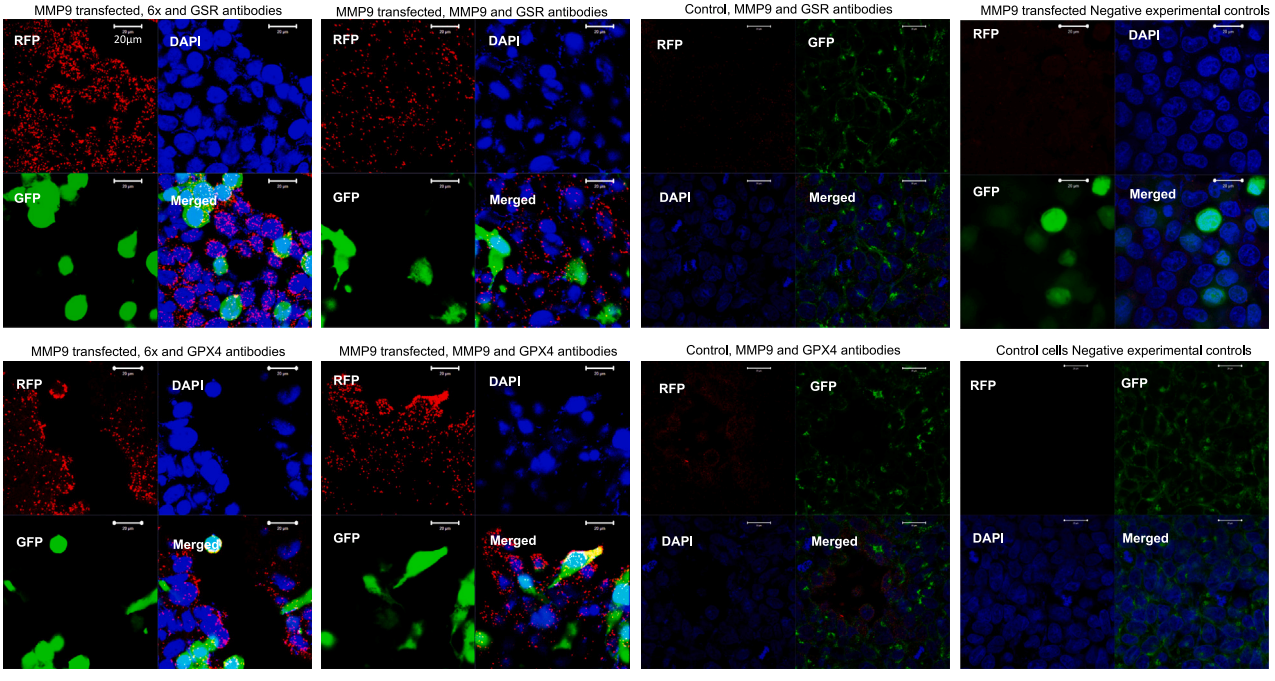


**Figure 2. MMP9 modulation of GPX4 and glutathione-based redox systems**

(A) GPX4 expression analysis: western blots reveal MMP9 overexpression leads to GPX4 downregulation, implicating MMP9 as a repressor of GPX4. In contrast, mutant MMP9 (MUT) does not exhibit this inhibitory effect.

(B) MMP9-GPX4 binding dynamics: coimmunoprecipitation demonstrates MMP9's interaction with GPX4, which is diminished in the MUT condition.

**Figure 2. *Continued***

(C) GPX4 activity assessment: GSH/GSSG ratios indicate MMP9 overexpression diminishes GPX4 activity, whereas MUT expression enhances it.

(D and E) GSSG and GSH quantification: elevated GSSG and unaltered GSH are observed with MMP9 overexpression, with MUT cells showing the increased GSH.

(F) GSR protein expression: western blot analysis reveals MMP9-mediated GSR reduction, critical for GSH regeneration from GSSG.

(G) MMP9-GSR interaction: coimmunoprecipitation confirms MMP9's affinity for GSR, reduced in the MUT variant.

(H) GPX1 expression impact: western blotting indicates MMP9 activity suppresses GPX1, a key player in cellular redox homeostasis. One-way ANOVA with Tukey's post hoc tests were applied for statistical validation from (A) to (H), with individual data points representing separate samples (n = 3–6). Data are presented as mean +/- standard deviation.

(I and J) Computational binding affinity predictions: *in silico* analyses predict strong binding affinities between MMP9-GSR (ΔG = −16.6 kcal/mol, Kd = 7.1E-13 M) and MMP9-GPX4 (ΔG = −13.8 kcal/mol, Kd = 7.1E-11 M), indicating potential regulatory interactions.

(K and L) MMP9 complex formation analysis: (1) ClusPro evaluations detail the stability of MMP9's interactions with GSR and GPX4, with weighted scores denoting complex robustness. (2) PRODIGY assessments elucidate the molecular interactions and potential functional implications of MMP9 with these complexes.

(M) Proximity ligation assay (PLA) visualization: confocal microscopy images (scale bar = 20 μm) exhibit red dots, marking the proximal interactions between MMP9 and GSR/GPX4 proteins. Negative control for PLA: control experiments, devoid of target proteins, confirm PLA specificity, as indicated by the absence of red signals, thereby ensuring the detected MMP9-related interactions are specific and reliable. *$p < 0.05$; **$p < 0.01$; ***$p < 0.001$; ****$p < 0.0001$; ns = not significant.

To determine how MMP9 regulates GPX4 activity, we measured the ratio of GSH to GSSG, where decreased GSH/GSSG ratio (depletion of GSH) suggests downregulated GPX4 activity. The glutathione (GSH) to glutathione disulfide (GSSG) ratio is a well-established and commonly employed indicator of GPX4 activity, as recommended in ferroptosis evaluation guidelines.[5,36,37] Typically, this ratio approximates 100:1 in most cells, although it can fluctuate across different models and in human patients.[38,39] Active MMP9 decreased while mutant MMP9 upregulated GPX4 activity (Figure 2C). The level of GSH/GSSG aligns with previous studies using the same kit.[37,40] The level of GSSG was increased in the MMP9-overexpressing cells, whereas GSH was increased in the mutant MMP9-expressing cells (Figures 2D and 2E). This finding demonstrated that expression and activity of MMP9 have opposite effects on GPX4 activity. Thus, MMP9 has a pivotal role in controlling GPX4 activity where active MMP9 downregulates while inactive MMP9 upregulates GPX4 activity.

Reduced GSH/GSSG ratio or GSH depletion could be either due to impaired conversion of GSSG into GSH (a quick replenishment mechanism of GSH to maintain GPX4 activity) or due to reduced biosynthesis of GSH by cysteine, which is imported through system xc− (mostly observed in a disease condition). As our experiments were conducted in normal (not diseased) cells, we measured the levels of GSR that reduces GSSG into GSH, replenishing GSH for sustained GPX4 activity.[4] GSR level was only decreased by the active MMP9 (Figure 2F), demonstrating that MMP9 activity is critical for downregulating GSR and inhibiting GPX4 activity. To ascertain MMP9's interaction with GSR, we conducted co-IP with MMP9-immunoprecipitated proteins. Our findings confirmed MMP9's binding to GSR (Figure 2G). This evidence points to MMP9 directly interacting with GSR to diminish its levels, with diminished MMP9 activity correlating to decreased binding efficiency, thereby preserving GSR levels.

GSR is also utilized by GPX1 to reduce hydrogen peroxide and soluble lipid hydroperoxide to maintain cellular redox level (Figure S5).[13] Immunoblotting showed that activity of MMP9 is critical for downregulating GPX1 (Figure 2H). Thus, MMP9 activity has pivotal roles in downregulating both GPX1 and GPX4 (Figures 2A and 2H) and their activities via GSR (Figure 2F) to disrupt cellular redox balance. These findings underscore MMP9's broader impact on cellular redox homeostasis through both GPX1 and GPX4 regulation.

As GSR replenishes GSH, which is at the crossroad of activity for both GPX4 and GPX1, we investigated the mechanism by which MMP9 regulates GSR. To investigate protein-protein interaction between GSR and MMP9, we performed *in silico* analysis using protein structures obtained from the Research Collaboratory for Structural Bioinformatics (RCSB) Protein Data Bank (PDB). We performed molecular docking of the protein structures of MMP9 (PDB:1L6J) and GSR (PDB: 3GRS) using the ClusPro 2.0 and the AutoDock software and determined predicted protein-protein binding affinity by the PRODIGY (Figures 2I and S3C). Similarly, we docked MMP9 with GPX4 (PDB: 6ELW) (Figure 2J). We selected the most energetically favorable orientations of MMP9 to its binding partner using ClusPro for docking. Subsequently, we utilized PRODIGY analysis to validate the docking results, measuring the protein-protein complex's binding affinity by calculating the binding free energy (ΔG) and the dissociation constant ($K_d$). The low values of ΔG and $K_d$ showed high binding affinity of MMP9 with GSR as well as with GPX4 (Figure 2L).[34,41] Furthermore, the Pymol and the ChimeraX programs were used to visualize and analyze the molecular interaction between MMP9 and GSR and between MMP9 and GPX4 (Figures 2I and 2J). We also substantiated the prediction between MMP9 and GSR by meticulously examining the bond lengths within the protein complex. Our analysis revealed that the intermolecular distances between MMP9 and GSR are within the range of 5.0 Å, indicative of strong noncovalent interactions typically observed in stable protein-protein complexes (Figures S6A and S6B; Video S2). These protein-protein interaction analyses along with the co-IP support that MMP9 directly binds to GSR and GPX4.

To determine interactions of MMP9 with GSR and GPX4 proteins within the cell, we performed proximal ligation assay (PLA), which visualizes proteins within the proximity of 40 nm.[42] We used non-transfected control cells and MMP9 plasmid-transfected cells and probed with either 6x-histidine tag (6x) or MMP9 with GSR antibody or no antibody (negative experimental control) (Figures S7A; Video S3 and S7C; Video S5). The presence of red dots in 6x and MMP9 with GSR antibody supports proximity of MMP9 with GSR (Figure 2M). Similarly, MMP9 and GPX4 proteins are in close proximity (Figure 2M). These results demonstrate a protein-protein interaction mechanism for MMP9-mediated regulation of GSR and GPX4.

The co-IP, protein-protein interaction, and PLA results collectively affirm MMP9's direct interaction with GPX4 and GSR. The observation that active MMP9 downregulates both GPX4 and GSR, with the mutant form of MMP9 showing no effect on these proteins, suggests that active MMP9 may facilitate their downregulation through proteolytic degradation. Furthermore, these insights unveil a mechanism by which MMP9 influences cellular redox balance, specifically through the modulation of GPX1, GPX4, and GSR, to regulate ferroptosis effectively.

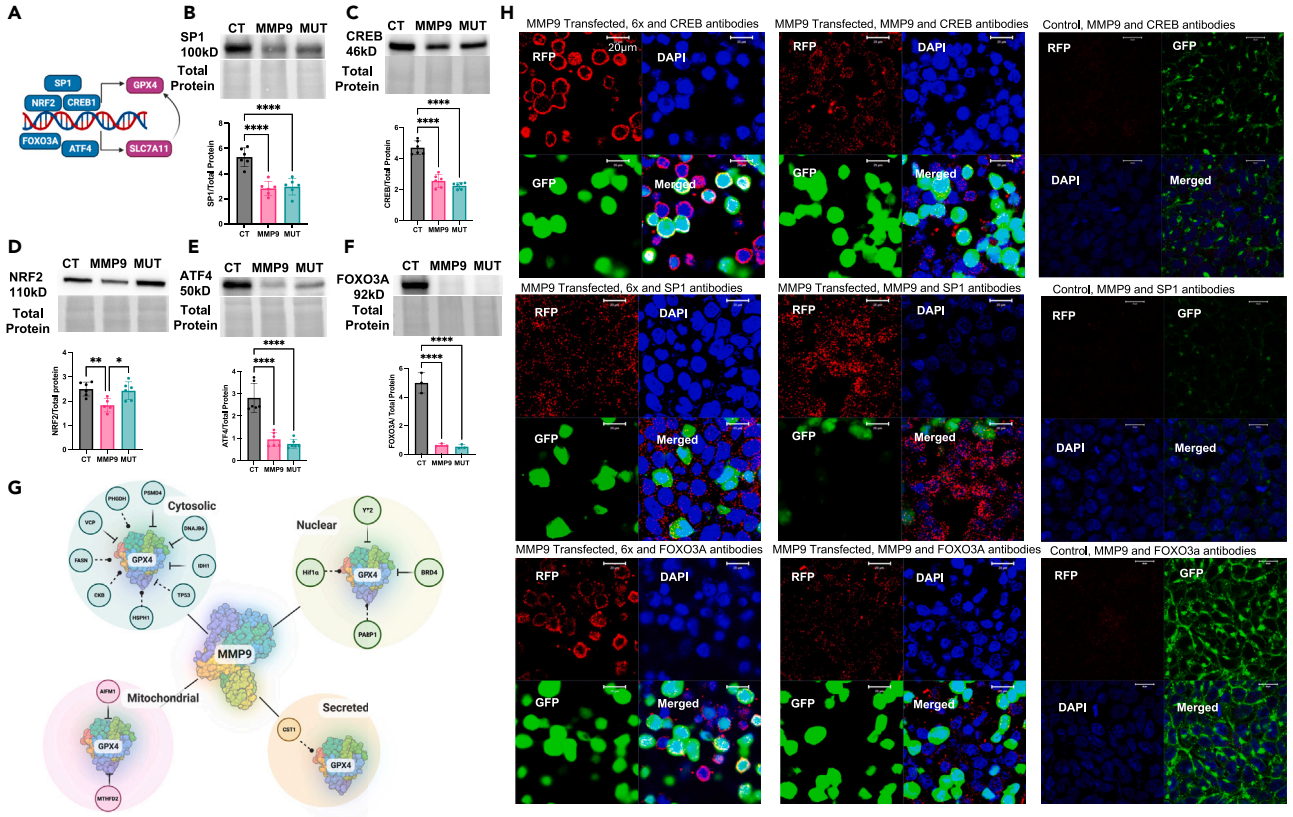


**Figure 3. MMP9-driven regulatory network affecting GPX4 transcriptional control**

(A) Regulatory schematic of GPX4 transcription: depiction of GPX4 regulation by five transcription factors: specificity protein-1 (SP1), cAMP response element-binding protein (CREB), and nuclear factor erythroid 2-related factor 2 (NRF2) directly influence GPX4 transcription. Forkhead box O3 (FOXO3) and activating transcription factor 4 (ATF4) modulate system xc− component solute carrier family 7 member 11 (SLC7A11), indirectly affecting GPX4 transcription.

(B and C) SP1 and CREB expression: western blot analyses show that MMP9 decreases SP1 and CREB levels, an effect observed with both active and inactive MMP9 variants.

(D) NRF2 expression: western blot results indicate that MMP9's enzymatic activity is crucial for downregulating NRF2.

(E and F) ATF4 and FOXO3 regulation: western blots demonstrate that MMP9 downregulates ATF4 and FOXO3, key regulators of SLC7A11, independent of its enzymatic activity. Data are presented as mean +/- standard deviation.

(G) MMP9's subcellular protein interactions: proteomic analysis via LC-MS/MS of MMP9-immunoprecipitated proteins identifies sixteen subcellular proteins that interact with MMP9, revealing a broad network through which MMP9 potentially modulates GPX4 expression.

(H) Visualization of transcription factor interactions: proximity ligation assay (PLA) displays interactions (red puncta) between MMP9 and the transcription factors CREB, SP1, and FOXO3, highlighting the molecular interplay influenced by MMP9. Scale bar = 10 μm. *$p < 0.05$; **$p < 0.01$; ****$p < 0.0001$.

## MMP9 downregulates GPX4 expression by controlling GPX4 transcription and subcellular localization

As the expression of GPX4 is downregulated by active MMP9, we sought to determine if MMP9 regulates GPX4 transcription. We measured the expression of the three key regulators of GPX4 transcription—nuclear factor SP1, CREB, and NRF2—and two nuclear factors that modulate GPX4 activity by controlling SLC7A11 (system xc−)—FOXO3 and ATF4 (Figure 3A). Both overexpressing and mutant MMP9 downregulated SP1 and CREB, suggesting that upregulated MMP9, independent of its activity, suppresses SP1 and CREB (Figures 3B and 3C). However, activity of MMP9 was crucial for downregulating NRF2 (Figure 3D). Notably, inactive MMP9 was unable to downregulate NRF2 (Figure 3D), suggesting that activity and not the expression of MMP9 is important for downregulating NRF2. The levels of ATF4 and FOXO3 were dramatically downregulated in both MMP9-overexpressing and mutant MMP9 groups (Figures 3E and 3F). This suggests a strong negative effect of MMP9, independent of its activity, on these two transcription factors.

Given GPX4's presence across various subcellular locales, we next explored MMP9's influence on subcellular GPX4 localization (Figures S4A and S4B).[43] To determine how MMP9 regulates subcellular GPX4, we used a rigorous method where MMP9 was immunoprecipitated and all proteins bound to MMP9 were assessed by LC-MS/MS proteomic analysis. We identified nine cytosolic, four nuclear, one secreted, and two mitochondrial proteins that directly bind to MMP9 (Figure 3G). Thus, MMP9 regulates GPX4 by directly binding to subcellular GPX4 and also by downregulating proteins that regulate GPX4 transcription and function. To validate if MMP9 is in proximity to proteins that regulate GPX4 transcription, we performed PLA on GPX4 transcription regulatory proteins. We observed that MMP9 was in proximity with CREB, SP1, and FOXO3, demonstrated by the presence of red puncta (Figures 3H and S7B; Video S4). Although our protein identification experiment did not

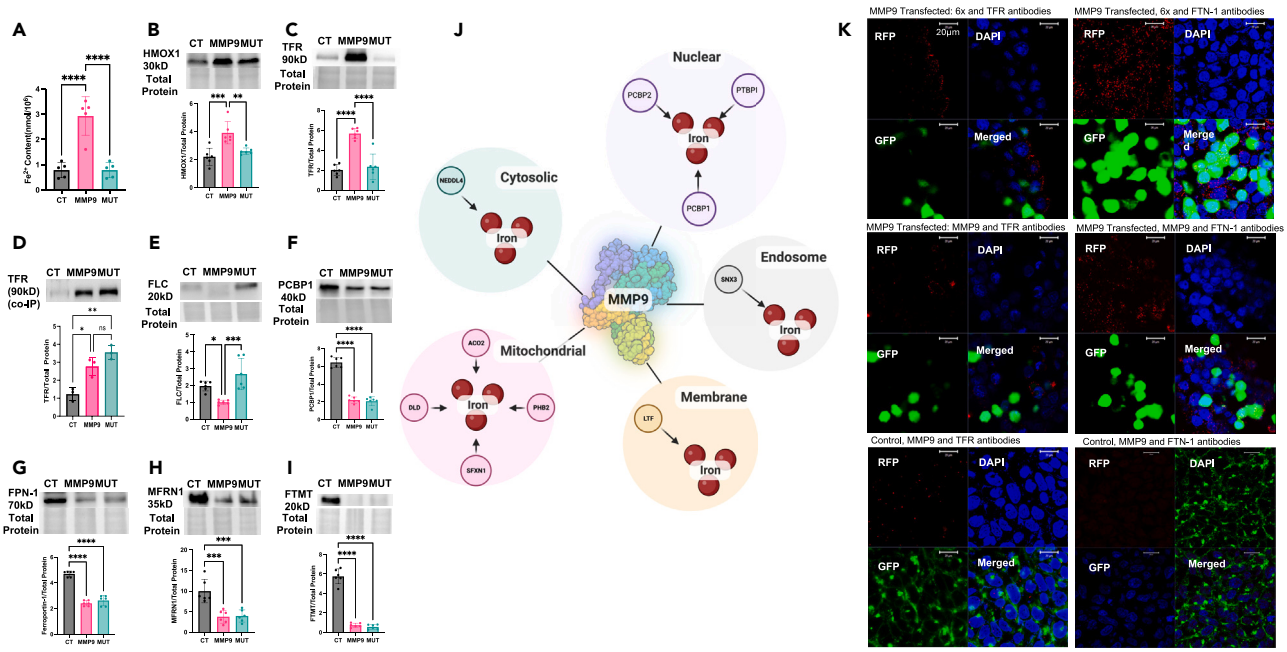


**Figure 4. MMP9 impairs iron homeostasis**

MMP9 upregulates redox-active ferrous iron ($Fe^{2+}$) by increasing iron metabolism and iron import and downregulating iron storage and export in HEK293 cells.

(A) Calorimetric measurement of $Fe^{2+}$ in untreated control (CT), MMP9 overexpressing (MMP9), and mutant (loss of collagenase activity) MMP9-expressing cells. Activity of MMP9 is essential for upregulation of $Fe^{2+}$.

(B) Western blotting of heme oxygenase-1 (HMOX1) enzyme that metabolizes heme to increase the levels of $Fe^{2+}$.

(C) Western blotting of transferrin receptor (TFR) showing activity of MMP9 is essential for the upregulation of TFR, which imports iron.

(D) Coimmunoprecipitation showing MMP9 binds to TFR Interaction.

(E) Western blotting of ferritin light chain (FLC) shows that active MMP9 downregulates FLC impairing iron storage.

(F) Western blotting of poly(rC)-binding protein 1 (PCBP1), a key protein in iron trafficking to storage sites, shows that MMP9 overexpression, irrespective of activity, downregulates PCBP1 to impair iron storage into ferritin.

(G) Western blotting of ferroportin-1 (FTN1) shows that increased levels of MMP9 downregulates FTN1 to impair iron export. Regulation of FTN1 is not dependent on MMP9 activity.

(H and I) Western blotting of mitoferrin-1 (MFRN1) that imports iron into mitochondria and mitochondrial ferritin (FTMT) that stores iron in mitochondria show that MMP9 overexpression, irrespective of activity, downregulates both MFRN1 and FTMT. Decreased levels of MFRN1 and FTMT suggest increased retention of cytosolic $Fe^{2+}$. From (A)–(I), data are presented as mean +/- standard deviation. One-way ANOVA followed by Tukey test was performed for statistical analysis. Each point represents one sample. n = 3–6.

(J) LC-MS/MS analysis of proteins immunoprecipitated with MMP9 reveals additional 10 subcellular proteins that bind to MMP9, suggesting a complex network by which MMP9 modulates iron homeostasis.

(K) Proximity ligation assays (PLAs) showing MMP9's interactions with TFR and FTN1. The presence of red puncta validates proximity of these proteins and suggests potential protein-protein interaction. Scale bar = 10 μm. *$p < 0.05$; **$p < 0.01$; ***$p < 0.001$; ****$p < 0.0001$.

demonstrate a direct interaction between MMP9 and GPX4 transcription factors, a plausible hypothesis for MMP9's modulation of these transcription factors could involve its indirect regulation. This regulation might occur either at the transcriptional level or through modulation of protein regulators associated with these transcription factors. Taken together, these findings illustrate that MMP9 orchestrates a sophisticated regulatory network to modulate GPX4, exerting its influence via transcription factors and an array of other regulatory proteins.

We also measured FSP-1 that suppresses ferroptosis through a GPX4-independent mechanism.[14,44] MMP9 overexpression, independent of its activity, downregulated FSP-1 (Figure S8A). Collectively, these findings illuminate MMP9's multifaceted role in inducing ferroptosis not only by downregulating GPX4 but also by engaging GPX4-independent mechanisms.

## MMP9 upregulates redox-active iron by impairing iron homeostasis

In the context of ferroptosis, redox-active ferrous iron ($Fe^{2+}$) serves as a crucial catalyst.[4] To determine the role of MMP9 in regulating cellular $Fe^{2+}$ levels, we performed colorimetric assay to measure $Fe^{2+}$ levels in cells overexpressing active (MMP9) and mutant MMP9 (MUT). Our results revealed that overexpression of active MMP9 elevated intracellular $Fe^{2+}$ levels, whereas the enzymatically inactive MMP9 did not provoke such an increase (Figure 4A). This suggests that MMP9's enzymatic activity is instrumental in the upregulation of $Fe^{2+}$.

The levels of $Fe^{2+}$ are increased by heme oxygenase-1 (HMOX1) enzyme, and knockdown of HMOX1 mitigates ferroptosis.[15,45] Therefore, we measured the levels of HMOX1 in the same groups. HMOX1 was upregulated only in the active MMP9 overexpressing group (Figure 4B).

Thus, activity of MMP9 is essential for upregulating HMOX1 and $Fe^{2+}$ levels. Impaired iron homeostasis may also upregulate $Fe^{2+}$. Thus, we investigated iron homeostasis by determining cellular iron import, iron storage, and export in the MMP9 overexpressing and mutant cells.

We determined iron import by measuring the levels of TFR. Active MMP9 increased TFR levels by 3-fold; however, mutant MMP9 has no effect on TFR levels (Figure 4C), suggesting that activity of MMP9 (and not the expression) is important for upregulating TFR.

To investigate MMP9's interaction with the TFR, we conducted co-IP across three groups: CT, MMP9 overexpression, and MUT. Our results confirmed MMP9's binding to TFR (Figure 4D). On further analysis on how PMA affects this interaction, we performed co-IP of TFR with MMP9 in the CT, MMP9, and MMP9+PMA groups. Both the MMP9 and MMP9+PMA groups demonstrated MMP9's binding to TFR, with the MMP9+PMA group showing a notably higher binding affinity than the MMP9 group (Figure S8B). This enhanced binding affinity suggests that PMA may contribute to the stabilization and subsequent upregulation of TFR.

The intracellular $Fe^{2+}$ concentration is modulated by storage in ferritin, with the ferritin light chain (FLC) playing an inhibitory role in ferroptosis.[18] We measured FLC levels and found that active MMP9 downregulated FLC, whereas the inactive MMP9 (MUT) did not (Figure 4E), underscoring the necessity of MMP9's activity in this regulatory process. Furthermore, the cytoplasmic iron chaperone PCBP1 facilitates $Fe^{2+}$ sequestration into ferritin.[19,46] Our data showed that both MMP9 overexpression and its mutant form suppressed PCBP1 levels (Figure 4F), suggesting a role for MMP9 in impeding $Fe^{2+}$ storage, independent of its activity. Additionally, we observed a decrease in ferritin heavy chain (FHC) levels induced by active MMP9 but not by MUT (Figure S8C).

The $Fe^{2+}$ level is also decreased by iron export through ferroportin-1 (FPN-1).[4] Therefore, we measured the levels of FPN-1 in the same experimental group. Both active and mutant MMP9 downregulated FPN-1 (Figure 4G), demonstrating that increased levels of MMP9, independent of its activity, suppresses FPN-1 to impair cellular iron export. Altogether these findings demonstrated that MMP9 has a key role in upregulating cellular $Fe^{2+}$ levels by increasing iron metabolism and import and decreasing iron storage and export.

Increased iron levels lead to lipid peroxidation in ferroptosis.[4] To assess lipid peroxidation, we measured malondialdehyde (MDA) levels, a key indicator of lipid peroxidation. Our findings show that MMP9 upregulates MDA, showing that MMP9 contributes to the induction of ferroptosis (Figure S9).

Altogether these findings demonstrated that MMP9 has a key role in upregulating cellular $Fe^{2+}$ levels by increasing iron metabolism and import and decreasing iron storage and export. Additionally, MMP9 promotes lipid peroxide accumulation, reinforcing its role in driving ferroptosis.

## MMP9 regulates mitochondrial iron regulatory proteins

Intracellular $Fe^{2+}$ concentrations, particularly within mitochondria, can be disrupted by the dysregulation of mitochondrial iron transport via mitoferrin-1 (MFRN1) and their storage in mitochondria in the form of mitochondrial ferritin (FTMT).[22,23] To elucidate MMP9's impact on these pathways, we quantified the levels of MFRN1 and FTMT across our experimental groups. We observed that MMP9 in both its active and mutant forms led to a suppression of MFRN1 and FTMT (Figures 4H and 4I), indicating that MMP9 modulates mitochondrial iron import and storage irrespective of its enzymatic activity. The pronounced decrease in FTMT levels particularly points to a significant role for MMP9 in curtailing mitochondrial iron sequestration.

To further unravel MMP9's role in subcellular iron regulation, we used MMP9 immunoprecipitated proteins for LC-MS/MS proteomic analysis. Our proteomic analysis revealed multiple proteins that interact with MMP9 involved in iron signaling. We mapped these proteins based on their subcellular localization. We identified one protein in cytosolic, membrane, and endosome, four proteins in mitochondria, and three proteins in nucleus that bind to MMP9 to regulate iron homeostasis (Figure 4J). These interactions suggest MMP9's extensive role in orchestrating the regulation of iron distribution within the cell.

## Validation of MMP9 interactions with iron-regulating proteins

To validate whether the MMP9 regulates iron homeostasis proteins, we performed PLA of MMP9 with iron importer TFR and iron exporter FPN1-1. We observed the red puncta in MMP9-treated TFR and FPN-1 (Figure 4K), demonstrating proximity of MMP9 with both TFR and FPN-1. The binding of MMP9 leads to either stabilization of protein, as occurred with TFR (Figures 4C and 4K), or degradation of protein, as occurred with FPN-1 (Figures 4G and 4K).

Altogether, these findings demonstrated that MMP9 regulates iron homeostasis through a direct protein-protein interaction, and binding of MMP9 with different iron homeostasis proteins may result in their upregulation or downregulation, plausibly through MMP9-induced stabilizing and proteolytic degradation, respectively.

## Identification of MMP9 subcellular binding partners to regulate ferroptosis

MMP9 regulates proteins in different subcellular organelles. To determine the subcellular roles of MMP9, we performed LC-MS/MS proteomic analysis on proteins immunoprecipitated with MMP9. We identified 83 subcellular proteins that bind with MMP9 (Table S1). The roles of these proteins in ferroptosis regulation are presented in Table 1. We have mapped these proteins based on their subcellular localization to further understand the dynamic function of MMP9 and the function of these proteins (Figure 5A). These novel MMP9-bound subcellular proteins are critical for comprehensive understanding of MMP9's intracellular regulatory roles. Furthermore, they are promising targets to uncover MMP9-mediated regulation of cellular mechanisms, including cell death via ferroptosis.

We developed a mutant MMP9 to demonstrate that MMP9 expression and activity have differential effects on cell cytotoxicity and ferroptosis regulatory pathways. We identified 83 subcellular proteins that bind with MMP9 (Figure 5A). Further studies on these proteins will reveal

**Table 1. LC-MS/MS derived MMP9 binding partners and their functions in ferroptosis**

| Protein names | Gene names | Function in ferroptosis | PMID |
|---|---|---|---|
| D-3-phosphoglycerate dehydrogenase/ Phosphoglycerate dehydrogenase | PHGDH | PHGDH impedes ferroptosis and fosters malignant progression through the upregulation of SLC7A11 in bladder cancer, indicating its role in cancer cell survival. | Shen et al.[47] |
| Membrane-associated progesterone receptor component 1 | PGRMC1 | The overexpression of PGRMC1 diminishes free iron levels and inhibits ferroptosis by binding intracellular iron; conversely, inhibiting PGRMC1 heightens the susceptibility of breast cancer cells to ferroptosis inducers. | Zhao et al.[48] |
| Sulfhydryl oxidase 1 | QSOX1 | QSOX1 sensitizes hepatocellular carcinoma cells to oxidative stress and augments the ferroptotic effects of sorafenib by downregulating NRF2, offering a potential therapeutic target. | Sun et al.[49] |
| Protein arginine N-methyltransferase 5 | PRMT5 | PRMT5 influences iron metabolism and engenders resistance to agents that induce ferroptosis, underscoring its role in cellular defence mechanisms. | Wang et al.[50] |
| Histone-lysine N-methyltransferase SETD1A | SETD1A | Through H3K4me3 methylation, SETD1A elevates the expression of lncRNA HOXC-AS3, which in turn stabilizes EP300 to attenuate ferroptosis in non-small cell lung cancer cells. | Shi et al.[51] |
| Transcription factor YY2 | YY2 | YY2 provokes ferroptosis in cancer cells and deters tumor growth by repressing SLC7A11 transcription, thus reducing glutathione synthesis and altering redox homeostasis. | Li et al.[52] |
| Prohibitin-2 | PHB2 | PHB2 contributes to the regulation of ferroptosis through a mechanism that is distinct from known signaling pathways. It achieves this regulation by modulating the expression of ferritin and ferritinophagy, which in turn influences the levels of ferritin and consequently the iron content within cells. | Yang et al.[53] |
| Sorting nexin-3 | SNX3 | SNX3 promotes ferroptosis by facilitating the recycling of the transferrin receptor, thereby disrupting iron homeostasis and augmenting iron accumulation, which can exacerbate cardiomyopathy induced by doxorubicin. | Lu et al.[54] |
| Bromodomain-containing protein 4 | BRD4 | BRD4 plays a protective role in defending DLBCL (diffuse large B-cell lymphoma) cells against ferroptosis by positively influencing the expression of FSP1 (ferroptosis suppressor protein 1). | Schmitt et al.[55] |
| DnaJ homolog subfamily B member 6 | DNAJB6 | In esophageal squamous adenocarcinoma, DNAJB6 overexpression accelerates glutathione degradation, downregulates GPX4, enhances lipid peroxidation, and promotes ferroptosis, demonstrating its contribution to the susceptibility of cancer cells to this form of cell death. | Jiang et al.[56] |

(*Continued on next page*)

**Table 1. *Continued***

| Protein names | Gene names | Function in ferroptosis | PMID |
|---|---|---|---|
| Vacuolar-protein-sorting-associated protein 4B | VPS4B | The ATPase activity of VPS4B, which dismantles the ESCRT-III complex post-membrane scission, is implicated in the iron dependency of cancer cells, making them more prone to ferroptosis | Hassannia et al.[57] |
| Isocitrate dehydrogenase (NADP) | IDH1 | Mutations in IDH1 attenuate GPX4 protein levels and deplete glutathione, thus promoting ferroptosis by reducing the cell's capacity to counteract lipid peroxidation. | Wang et al.[58] |
| Apoptosis-inducing factor 1 | AIFM1 | Mitochondrial oxidative damage leads to the release of AIFM1, which promotes ferroptosis by translocating to the nucleus. Additionally, the STING1-MFN1/2 pathway initiates ferroptosis by promoting mitochondrial fusion, resulting in increased ROS production. | Chen et al.[59] |
| Cystatin-SN; cystatin-S | CST1; CST4 | CST1 hinders the ubiquitination of GPX4 by engaging OTUB1, which enhances GPX4 stability and decreases intracellular reactive oxygen species, consequently inhibiting ferroptosis and facilitating metastasis in gastric cancer. | Li et al.[60] |
| Lactotransferrin | LTF | Lactotransferrin (LTF) acts as a facilitator of ferroptosis by enhancing the uptake of iron. | Tang et al.[61] |
| Catalase | CAT | Catalase upregulation has been associated with increased resistance to ferroptosis in specific cell types and offers cardioprotective effects against oxidative stress by mitigating ferroptosis. | Zhang et al.[62] |
| Glyceraldehyde-3-phosphate dehydrogenase | GAPDH | Lowered expression of GAPDH in tumors decelerates the glycolytic pathway, disrupting the energy metabolism of the tumor and consequently intensifying tumor cell death triggered by ferroptosis. | Ouyang et al.[63] |
| Cellular tumor antigen p53 | TP53 | This protein acts as a guard against cancer, commonly mutated in various cancers, including lung cancer. It is a key regulator of both programmed cell death and a specific type called ferroptosis, where iron plays a role. TP53 works to halt lung cancer growth by triggering this iron-dependent cell death process. | Jiang et al.[64] |
| Protein S100-A8; Protein S100-A8, N-terminally processed | S100A8 | S100A8 is involved in controlling autophagy-dependent ferroptosis in microglia following experimental subarachnoid hemorrhage. | Tao et al.[65] |
| Keratin, type I cytoskeletal 18 | KRT18 | Keratin 18 is implicated in regulating both apoptosis (a form of programmed cell death) and ferroptosis, especially after cells are exposed to low oxygen pressure environments. It may act through a specific cell signaling pathway known as JNK. | Cui et al.[66] |

(*Continued on next page*)

**Table 1. *Continued***

| Protein names | Gene names | Function in ferroptosis | PMID |
|---|---|---|---|
| Cyclin-dependent kinase 1 | CDK1 | CDK1 directly phosphorylates and ubiquitinates the ACSL4 protein, leading to the degradation of ACSL4. This process inhibits ferroptosis and enhances resistance to oxaliplatin. | Zeng et al.[67] |
| Alpha-enolase | ENO1 | ENO1 suppresses ferroptosis in cancer cells by facilitating the degradation of iron regulatory protein 1 (IRP1) mRNA. | Zhang et al.[68] |
| Fumarate hydratase | FH | An enzyme in the energy-producing cycle of cells, its genetic mutation is linked to a hereditary cancer syndrome and causes cell death via ferroptosis when inactivated. | Liu et al.[22] |
| 4F2 cell-surface antigen heavy chain/Solute carrier family 3 member 2 | SLC3A2 | It appears that SLC3A2 hinders ferroptosis, in part, through a pathway that involves mTOR, which is a central regulator of cell growth and survival. | Wu et al.[69] |
| Vimentin | VIM | Required for the rapid expansion and spread of lung cancer, it also protects these cells from dying via ferroptosis. | Berr et al.[70] |
| Glutathione S-transferase P/Glutathione S-transferase Pi 1 | GSTP1 | GSTP1 facilitates the conversion of intracellular reactive oxygen species and hydroxyl radicals by catalyzing their reaction with glutathione, thus preventing the oxidation of polyunsaturated fatty acids on the cell membrane and combating ferroptosis. | Tan et al.[71] |
| Dihydrolipoyl dehydrogenase, mitochondrial | DLD | Stimulated by a metabolic intermediate called αKG, this enzyme helps increase local iron levels and produce molecules that promote ferroptosis, especially under conditions where cells are deprived of an amino acid called cystine. | Tang et al.[61] |
| Poly [ADP-ribose] polymerase 1 | PARP1 | Inhibition of PARP promotes ferroptosis by suppressing the expression of SLC7A11 and works in synergy with ferroptosis-inducing agents in ovarian cancer cases with intact BRCA function. | Hong et al.[72] |
| Thioredoxin | TXN | Thioredoxin-1 mitigates MPP+/MPTP-induced ferroptosis by elevating the levels of glutathione peroxidase 4 (GPX4). | Bai et al.[73] |
| Creatine kinase B-type | CKB | Creatine kinase B inhibits ferroptosis by phosphorylating GPX4. | Wu et al.[74] |
| Protein disulfide-isomerase A4 | PDIA4 | PDIA4 counteracts ferroptosis by modulating the ER stress regulatory pathway involving PERK/ATF4 and the downstream protein SLC7A11. | Kang et al.[75] |
| Prolyl 4-hydroxylase subunit alpha-1 | P4HA1 | P4HA1 activates HMGCS1, which in turn promotes ferroptosis resistance and disease progression in nasopharyngeal carcinoma. | Zhou et al.[76] |
| Methylenetetrahydrofolate dehydrogenase (NADP+ dependent) 2, methenyltetrahydrofolate cyclohydrolase | MTHFD2 | The knockdown of MTHFD2 in ferroptosis led to increased intracellular ROS, lipid peroxidation, reduced GSH levels, and down-regulation of SLC7A11, GPX4, and NRF2 expressions. | Zhang et al.[77] |

(*Continued on next page*)

**Table 1. *Continued***

| Protein names | Gene names | Function in ferroptosis | PMID |
|---|---|---|---|
| Macrophage migration inhibitory factor | MIF | Inhibits ferroptosis of macrophages, functional inhibitors cause downregulation in GPX4, and recombinant factor of MIF restores the expression of GPX4 | Cai et al.[78] |
| Heterogeneous nuclear ribonucleoprotein L | HNRNPL | HnRNPL suppresses ferroptosis in castration-resistant prostate cancer (CRPC) cells mediated by Jurkat T cells by involving the YY1/PD-L1 pathway. | Dang et al.[79] |
| Glutathione S-transferase Mu 5; Glutathione S-transferase Mu 2; Glutathione S-transferase Mu 3 | GSTM5; GSTM2; GSTM3 | Involved in glutathione metabolism | Zhang et al.[80] |
| Voltage-dependent anion-selective channel protein 1 | VDAC1 | The activation of VDAC, which facilitates the passage of the majority of metabolites into the mitochondria, leads to an enhancement in mitochondrial metabolism and the generation of reactive oxygen species (ROS). Calcium ions (Ca2+) enter the mitochondria via VDAC, thereby playing a role in the generation of ROS. | Wu et al.[81] |
| Ubiquitin-like modifier-activating enzyme 1 | UBA1 | Blocking UBA1 hampers the growth, movement, and infiltration abilities of hepatocellular carcinoma (HCC) cells. Additionally, when UBA1 is inhibited, there is an increase in both iron levels and malondialdehyde (MDA) concentrations. | Wang et al.[82] |
| Transcriptional repressor protein Yin Yang 1 | YY1 | YY1 decreases the levels of SIRT1 by obstructing its transcription, leading to the induction of ferroptosis in synoviocytes induced by LPS | Zhan et al.[83] |
| Polypyrimidine tract-binding protein 1 | PTBP1 | PTBP1 is involved in ferroptosis in liver cancer via regulating NCOA4 translation, which is a regulator of ferritinophagy. | Yang et al.[84] |
| Mitogen-activated protein kinase 1 | MAPK1 | The MAPK pathway is significantly involved in ferroptosis, with previous research suggesting that lipid ROS activates the p38 MAPK pathway, contributing to ferroptosis, and studies also confirmed that the activation of the MAPK/ERK pathway is necessary for erastin-induced ferroptosis in PDAC cells. | Song et al.[85] |
| Peroxiredoxin-6 | PRDX6 | Reducing the levels of PRDX6 through knockdown greatly intensifies the accumulation of lipid peroxides (LOOH) and the resulting ferroptotic cell death when exposed to ferroptosis-inducing agents across different cancer cell lines. Conversely, augmenting PRDX6 levels through overexpression mitigates the generation of LOOH and the subsequent cell death triggered by erastin-induced ferroptosis. | Lu et al.[86] |

(*Continued on next page*)

**Table 1. *Continued***

| Protein names | Gene names | Function in ferroptosis | PMID |
|---|---|---|---|
| S-adenosylmethionine synthase isoform type-2/methionine adenosyltransferase 2A | MAT2A | MAT2A facilitates the synthesis of S-adenosylmethionine (SAM), which, in turn, elevates ACSL3 expression by enhancing trimethylation of lysine-4 on histone H3 (H3K4me3) within the promoter region. This ultimately leads to the development of resistance against ferroptosis. | Ma et al.[87] |
| Peroxiredoxin-2 | PRDX2 | PRDX2 is responsible for mediating the inhibitory effects of ISO (Isocitrate) treatment on ferroptosis by reducing oxidative stress, preventing iron overload, and decreasing lipid peroxidation. | Chen et al.[88] |
| Cyclin-dependent kinase inhibitor 2A | CDKN2A | CDKN2A serves as a crucial controller of lipid composition and safeguards against the initial stages of ferroptosis in glioblastoma multiforme (GBM) by modifying the acyl tail composition and redirecting fatty acids into triacylglycerols (TAGs) stored within lipid droplets. | Minam et al.[89] |
| Voltage-dependent anion-selective channel protein 2 | VDAC2 | The suppression of VDAC2 or VDAC3 has a substantial inhibitory effect on ferroptotic processes triggered by erastin. This inhibition encompasses reduced production of lipid-derived reactive oxygen species (ROS), diminished iron accumulation, depletion of glutathione (GSH), and decreased generation of glutathione disulfide (GSSG). | Yang et al.[90] |
| Isocitrate dehydrogenase | IDH2 | IDH2 plays a role in modulating the assembly of the matrix domain of complex I (CI) and, consequently, the entire oxidative phosphorylation (OXPHOS) system, while also regulating ferroptosis, the mitochondrial unfolded protein response, and OXPHOS assembly in Drosophila. | Murari et al.[91] |
| Fatty acid synthase | FASN | The upregulation of HIF1α by PRDX4 leads to its increased nuclear translocation, stabilizes its protein structure, and inhibits ubiquitin-induced degradation, ultimately resulting in the upregulation of SLC7A11 expression. FASN binds to HIF1a and antagonizes SLC7A11-mediated ferroptosis resulting in sorafenib resistance. | Li et al.[92] |
| T-complex protein 1 subunit gamma | CCT3 | CT3 plays a role in promoting the proliferation and growth of lung cancer cells by inhibiting ferroptosis and activating the EGFR and AKT pathways. | Wang et al.[93] |

(*Continued on next page*)

**Table 1. *Continued***

| Protein names | Gene names | Function in ferroptosis | PMID |
|---|---|---|---|
| Ras-related protein Rab-7a | RAB7A | RAB7A belongs to the RAS oncogene family and acts as a cargo receptor essential for the process of lipophagy. Lipophagy is responsible for the specific identification and degradation of lipid droplets, which in turn leads to increased production of free fatty acids, the promotion of lipid peroxidation, and the initiation of ferroptosis. | Chen et al.[94] |
| 26S proteasome non-ATPase regulatory subunit 4 | PSMD4 | PSMD4, which functions as a receptor for ubiquitin in the proteasome, plays a crucial role in facilitating the degradation of GPX4, leading to the initiation of ferroptosis. Therefore, hindering the PSMD4-dependent degradation of GPX4 effectively prevents trypsin-enhanced ferroptosis in acinar cells. | Liu et al.[95] |
| Transitional endoplasmic reticulum ATPase/ Valosin-containing protein | VCP | The repositioning of VCP (valosin-containing protein) restricts mitochondrial function, prevents the depletion of glutathione (GSH), and hinders ferroptosis in PC3 prostate cancer cells when subjected to starvation conditions. | Ogor et al.[96] |
| Myelin proteolipid protein/Proteolipid protein 1 | PLP1 | PLP1 displays significant characteristics associated with ferroptosis, including increased levels of lipid peroxidation, elevated production of reactive oxygen species (ROS), disrupted iron metabolism, and heightened sensitivity to free iron. | Nobuta et al.[97] |
| 40S ribosomal protein S7 | RPS7 | Promotes ferroptosis in cisplatin-treated BUMPT cells. | Zhang et al.[98] |
| High density lipoprotein-binding protein | HDLBP | HDLBP inhibits the ferroptosis vulnerability of HCC by stabilizing LncFAL. Splicing of LncFAL is increased by YTHDF2 in a m6A-dependent manner in HCC. LncFAL inhibits FSP1 polyubiquitination by disrupting the FSP1-TRIM69 interaction. FSP1 blockade is essential for the induction of ferroptosis in HCC. | Yuan et al.[99] |
| Mitochondrial 2-oxoglutarate/malate carrier protein/Solute Carrier Family 25 member 11 | SLC25A11 | Regulates mitoGSH for GPX4 function and stability. | Ta et al.[100] |
| Single-stranded DNA-binding protein | SSBP1 | SSBP1 interacts with p53 and promotes the phosphorylation of p53 at the S15 position, which in turn leads to an increased accumulation of nuclear p53 in glomerular podocytes undergoing ferroptosis when exposed to high fructose stimulation. | Wu et al.[101] |
| Proteolipid protein 2 | PLP2 | Involved in lipid accumulation | Guo et al.[102] |
| Peroxiredoxin-1 | PRDX1 | PRDX1 is essential for regulating the reaction of CEnCs to substances that induce lipid peroxidation. | Lovatt et al.[103] |
| Peroxiredoxin-4 | PRDX4 | Suppresses ferroptosis through antioxidant effects | Luo et al.[104] |

(*Continued on next page*)

**Table 1. *Continued***

| Protein names | Gene names | Function in ferroptosis | PMID |
|---|---|---|---|
| Ras GTPase-activating protein-binding protein 1 | G3BP1 | Ras GTPase-activating protein-binding protein 1 (G3BP1) is located within lysosomes, where it plays a crucial role in orchestrating lysophagy primarily through the G3BP1/TSC2 complex. When the G3BP1/TSC2 complex malfunctions, it leads to an acceleration of lysosomal damage and promotes ferroptosis in NP (nucleus pulposus) cells. | Li et al.[105] |
| Sequestosome-1 | SQSTM1 | P62/SQSTM1 has the ability to suppress ferroptosis by activating the NRF2 signaling pathway. | Yuan et al.[106] |
| Poly(rC)-binding protein 1 | PCBP1 | PCBP1 represses ferritinophagy-mediated ferroptosis | Lee et al.[107] |
| Poly(rC)-binding protein 2; Poly(rC)-binding protein 3 | PCBP2; PCBP3 | PCBP2 delivers Fe2+ to ferritin, resulting in the suppression of ferroptosis | Frey et al.[108] |
| ELAV-like protein 1 | ELAVL1 | The introduction of ELAVL1 siRNA resulted in resistance to ferroptosis, while the ELAVL1 plasmid promoted the occurrence of typical ferroptotic events. Intriguingly, elevated levels of ELAVL1 expression also seemed to enhance the generation of autophagosomes and the overall macroautophagic/autophagic flux, which constituted the underlying mechanism responsible for the enhanced ferroptosis induced by ELAVL1. | Zhang et al.[109] |
| Coiled-coil domain-containing protein 6 | CCDC6 | The depletion of CCDC6 is linked to increased expression levels of xCT, which in turn results in heightened tolerance to oxidative stress and resistance to ferroptosis in testis germ cells. | Morra et al.[110] |
| RNA demethylase/alkB homolog 5 | ALKBH5 | ALKBH5 plays a role in promoting ferroptosis in hypopharyngeal squamous cell carcinoma by suppressing the expression of Nrf2 through a mechanism that depends on m6A-IGF2BP2. Specifically, ALKBH5 demethylates m6A sites located in the 3′-UTR of Nrf2 mRNA, leading to its reduced expression and ultimately contributing to ferroptosis in this context. | Chen et al.[111] |
| Protein LYRIC/Metadherin | MTDH | MTDH (Metadherin) amplifies the capacity of breast cancer cells to utilize intracellular glutamate to sustain respiratory chain activity. This process has been shown to be a crucial metabolic mechanism that promotes ferroptosis in these cells. | Li et al.[112] |
| Protein FAM98A | FAM98A | FAM98A, a microtubule-associated protein, participates in cell proliferation and migration. Elevated levels of FAM98A expression have the potential to impede ferroptosis and enhance resistance of colorectal cancer (CRC) cells to the effects of 5-fluorouracil (5-FU). | He et al.[113] |
| Putative RNA-binding protein 15B | RBM15B | The suppression of RBM15 leads to an increase in ferroptosis by influencing the TGF-β/Smad2 pathway in lung cancer. | Feng et al.[114] |

(*Continued on next page*)

**Table 1. *Continued***

| Protein names | Gene names | Function in ferroptosis | PMID |
|---|---|---|---|
| Protein NDRG1 | NDRG1 | The hub gene NDRG1, which is associated with the response to TACE (transarterial chemoembolization), appears to function as a protector against ferroptosis, contributing to the development of tumorigenesis and metastasis in hepatocellular carcinoma (HCC). | Tang et al.[115] |
| Heat shock protein 105 kDa/Heat shock protein family H | HSPH1 | HSF1 appears to have a crucial role in protecting cardiomyocytes against ferroptosis induced by palmitic acid (PA). It does so by preserving cellular iron balance and ensuring the expression of GPX4, which is essential in mitigating ferroptosis. | Wang et al.[116] |
| Transcription factor GATA-6 | GATA6 | GATA6, in the context of cerebral ischemia-reperfusion injury, acts to suppress neuronal autophagy and ferroptosis. It accomplishes this through a mechanism that relies on the miR-193b/ATG7 axis, which plays a critical role in mediating its effects. | Fan et al.[117] |
| FAS-associated factor 2 | FAF2 | The molecule Fas-associated factor family member 2 (FAF2), which plays a role in the regulation of lipid droplet (LD) formation and maintenance, is observed to be downregulated in orlistat-induced ferroptosis in A549 and H1299 lung cancer cells. | Zhou et al.[118] |
| E3 ubiquitin-protein ligase NEDD4-like | NEDD4L | A regulator of GPX4 stability | Cheng et al.[119] |
| Putative RNA-binding protein 15 | RBM15 | The suppression of RBM15 leads to an increase in ferroptosis by modulating the TGF-β/Smad2 pathway in lung cancer. | Feng et al.[114] |
| Protein deglycase DJ-1 | PARK7 | Park7, also known as DJ-1, counteracts iron overload by controlling the transcription of the iron regulatory protein family and simultaneously preventing excessive iron uptake by mitochondria. | Pan et al.[120] |
| Aconitate hydratase/ACO2 aconitase 2 | ACO2 | The presence of ACO2 (Aconitase 2) was observed to play a role in the regulation of cellular iron levels. Specifically, elevated expression of ACO2 led to an increase in the translation factors known as iron response element binding protein 1 (IREB1), which are involved in the control of iron metabolism. | Mirhadi et al.[121] |
| Egl nine homolog 1/Hypoxia-inducible factor prolyl hydroxylase 2 | EGLN1 | The combination of EGLN1 and c-Myc induces the expression of a lymphoid-specific helicase that, in turn, hinders ferroptosis by altering the expression of genes involved in lipid metabolism. | Jiang et al.[122] |
| Sideroflexin-1 | SFXN1 | SFXN1, which is a multi-spanning transmembrane protein situated in the inner mitochondrial membrane, has a critical function in facilitating the transport of iron into the mitochondria. | Sun et al.[123] |

(*Continued on next page*)

**Table 1. *Continued***

| Protein names | Gene names | Function in ferroptosis | PMID |
|---|---|---|---|
| MICOS complex subunit MIC19/Coiled-coil-helix-coiled-coil-helix domain containing 3 | CHCHD3 | CHCHD3 functions in ferroptosis by enhancing mitochondrial function and contributing to the elevation of mitochondrial reactive oxygen species (ROS) levels during the process. | Xue et al.[124] |
| CDGSH iron-sulfur domain-containing protein 1 | CISD1 | CISD1 prevents ferroptosis by shielding mitochondria from lipid peroxidation. | Yuan et al.[125] |
| Vacuolar protein sorting-associated protein 4A | VPS4A | Dysregulation or deficiency of VPS4 can affect various cellular death processes, including pyroptosis and ferroptosis. Additionally, dysfunctional VPS4 can reduce the ability to repair membrane damage, increasing the likelihood of ferroptosis in cancer cells. | Huang et al.[126] |

the comprehensive molecular mechanisms regulated by subcellular MMP9. We have uncovered key mechanisms by which intracellular MMP9 downregulates GPX4 expression and activity and upregulates $Fe^{2+}$ to induce ferroptosis (Figure 5B).

To explore the role of MMP9 in the regulation of ferroptosis, we conducted a series of integrated pathway analyses (IPAs). These analyses were designed to dissect the molecular consequences of MMP9 modulation on the complex network of ferroptosis signaling. Using computational IPA, we examined the activation effects of MMP9 on ferroptosis. The activation of MMP9 was found to have widespread implications on the regulatory landscape of ferroptosis, affecting both direct and indirect modulators of this cell death pathway. The upregulation of active MMP9 resulted in the engagement of multiple signaling molecules that have been previously implicated in the initiation and progression of ferroptosis, suggesting that MMP9 acts as an upstream effector in this intricate cellular cascade (Figure 6A). Conversely, the inhibitory effects of MMP9 on ferroptosis signaling were also assessed. The suppression of MMP9 function delineated an alternate set of molecular interactions, which seemingly counteracted the pro-ferroptotic signals (Figure 6B). This portion of the analysis provided insights into how MMP9 inhibition could potentially stabilize cellular mechanisms that deter ferroptosis, highlighting a complex interplay where MMP9 serves as a bidirectional modulator of this specialized form of cell death.

The results of our IPA offer a roadmap for future investigations into the nuanced roles of MMP9 within the ferroptosis pathway. By pinpointing specific molecules and interactions influenced by MMP9 activity, this study lays the groundwork for further exploration into the therapeutic potential of MMP9 modulation. By delineating the activation and inhibition spectra of MMP9 within ferroptosis signaling, we open avenues for understanding how ferroptosis can be precisely controlled by MMP9.

## DISCUSSION

Although ferroptosis has important role in many diseases, its molecular mechanisms remain unclear.[2] Our study sheds light on this by identifying MMP9 as a novel inducer of ferroptosis. We have delineated the mechanisms by which MMP9 suppresses GPX4 and elevates $Fe^{2+}$ levels, key factors in ferroptosis induction.[4,5] MMP9 downregulates GPX4 by directly interacting with GPX4 protein and by modulating five transcription regulators: SP1, CREB1, NRF2, ATF4, and FOXO3. Furthermore, MMP9 suppresses the activity of GPX4 by decreasing the levels of GSR potentially through a protein-protein interaction. This action of MMP9 represents a multifaceted regulatory approach, encompassing both the downregulation of GPX4 expression and the suppression of its activity, thereby influencing a broad spectrum of intracellular GPX4 signaling pathways. We show the presence of subcellular MMP9 and identified at least 83 intracellular proteins that bind to MMP9 and regulate ferroptosis pathways. The computational IPA with MMP9 activation as well as MMP9 inhibition show how MMP9 potentially modulates ferroptosis signaling pathways. Thus, MMP9 has a pivotal role in the regulation of ferroptosis.

MMP9 also regulates GPX4-independent mechanisms to impair cellular redox balance to promote ferroptosis. MMP9 suppresses GPX1, which reduces oxidative radicals to maintain cellular redox balance. By reducing GSR, MMP9 also downregulates GPX1 activity. MMP9 also inhibits FSP-1, which is a newly discovered suppressor of ferroptosis. Thus, MMP9 inhibits GPX4-dependent and GPX4-independent mechanisms to induce ferroptosis.

MMP9 induces ferroptosis by increasing the levels of $Fe^{2+}$. It upregulates HMOX1 to release iron from heme. It also deranges iron homeostasis by upregulating iron import and downregulating iron storage and export, which results in upregulation of $Fe^{2+}$. Besides ferroptosis, iron plays a crucial role in many cellular functions.[127] Thus, MMP9's regulation of iron homeostasis is critical for several cellular function. In addition, loss of MMP9 is demonstrated to improve cell viability by suppressing oxidative stress and inflammation.[29] MMP9 also increases the accumulation of lipid peroxides, supporting its role in ferroptosis. Altogether, these findings demonstrate that MMP9 has pivotal roles in intracellular redox balance, iron homeostasis, and cell death via ferroptosis.

MMP9 being a secretary protein is least studied for the intracellular functions. The presence of MMP9 in subcellular locations like mitochondria[128,129] and the nucleus[130] has been established, along with its role in epigenetic regulation and autophagy, underscoring its intracellular functions.[30] Except few reports on intracellular functions of MMP9,[30,34] the intracellular and subcellular functions of MMP9 are unknown. We validated the subcellular localization of MMP9 and revealed 83 subcellular proteins that bind to MMP9. In addition to nucleus

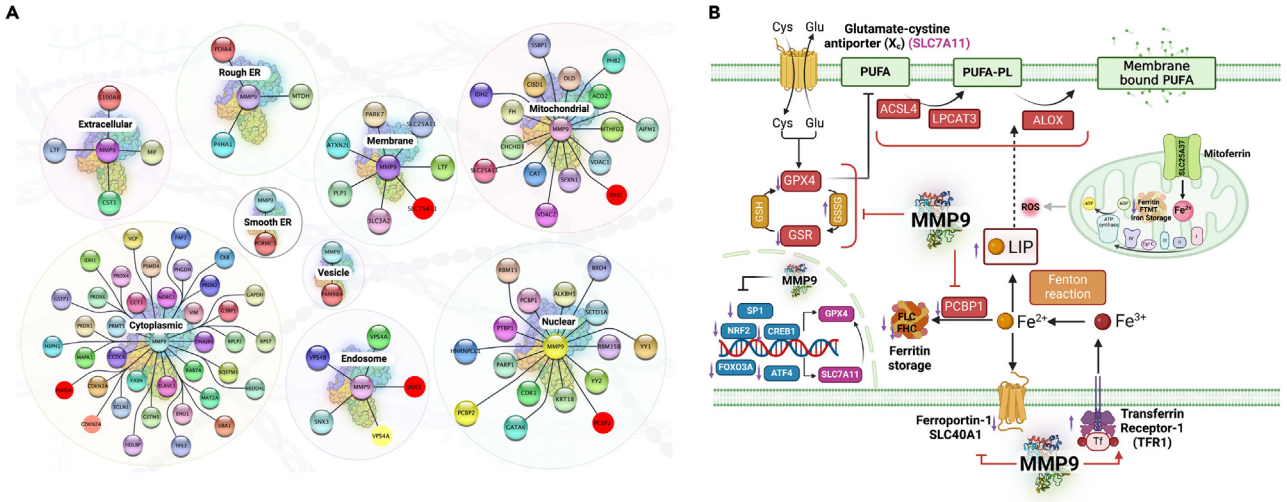


**Figure 5. MMP9's regulatory network in ferroptosis pathways**

(A) Discovery of MMP9-associated proteins: LC-MS/MS analysis of MMP9-immunoprecipitated proteins has identified 83 novel proteins within various subcellular compartments, indicating MMP9's broad scope of influence. Cytoscape visualization quantifies the interactions, shedding light on MMP9's extensive subcellular reach.

(B) MMP9's central role in ferroptosis signaling: integrating data from preceding figures, a schematic underscores MMP9 as a pivotal regulator in the ferroptosis signaling cascade. Detailed are MMP9's interactions with principal iron regulatory proteins including transferrin receptor 1 (TFR), ferroportin-1 (FPN1), and ferritin light chain (FLC), which are integral to iron homeostasis. Additionally, the diagram delineates MMP9's impact on GPX4, both through direct binding and indirect transcriptional control via SP1, NRF2, CREB1, as well as FOXO3 and ATF4, leading to downstream modulation of system xc– (through SLC7A11) and affecting glutathione-based antioxidant systems. These pathways highlight MMP9's ability to modulate ferroptosis through dual pathways of iron regulation and lipid peroxide detoxification. MMP9's broad regulatory influence as depicted underscores its therapeutic potential in conditions characterized by dysregulated ferroptosis.

and cytoplasm, the presence of MMP9 binding proteins in endoplasmic reticulum (ER), endosomes, vesicle, membrane, and mitochondria suggest that MMP9 has multifarious regulatory role in subcellular functions. Our findings provide a platform for future studies to determine the comprehensive roles of MMP9 in intracellular signaling mechanisms.

We used a unique approach to identify the specific binding partners of subcellular MMP9, where we used MMP9 immunoprecipitated proteins for LC-MS/MS proteomic analysis. This approach rules out any non-MMP9 binding protein, which is common in proteomic analysis of cells. The Cytoscape/String analysis of MMP9 binding proteins in subcellular compartments are valuable to determining the effect of subcellular MMP9 in different disease conditions and diagnosing the cause for MMP9-mediated diseases.

There is limited knowledge on non-enzymatic functions of MMP9. We developed a collagenase mutant MMP9, which is structurally similar to normal MMP9. Transfection of this mutant MMP9 increases the expression but not the collagenase activity of MMP9. We also used gain-of-MMP9 function by overexpressing and activating MMP9. This loss- and gain-of-function of MMP9 studies provide an excellent approach to delineate the cellular effects of expression versus activity of MMP9.

MMP9 has been a promising therapeutic target for cancer.[131] Recent studies raise hopes for MMP9 inhibitors; however, a deeper understanding of MMP9-regulated mechanisms is warranted.[132] In cardiac diseases, MMP9 induces pathogenesis and is associated with human heart failure, and ablation of MMP9 has cardioprotective effects.[3,133–135] Our findings provide a comprehensive list of novel subcellular proteins regulated by MMP9, which will elucidate the intracellular regulatory roles of MMP9 and help developing therapeutic targets for MMP9-induced cardiac diseases.

We used human embryonic kidney 293 (HEK293) cells and cultured them in a serum-free medium. HEK293 is transfection-efficient cells with biotherapeutic value.[35] Thus, it will be easy to utilize our findings for translational studies. We did not use a disease model, which may have confounding effects in signaling pathways. Thus, the effects observed in the signaling pathways and molecules are purely due to change in MMP9 expression and activity.

In summary, we reveal a role of subcellular MMP9 in regulation of redox balance and iron homeostasis to induce ferroptosis signaling. Our newly identified subcellular MMP9-regulated proteins will move the field of MMP9 biology forward to understand the cellular functions of MMP9, understand the subcellular changes in MMP9 in a disease condition, and potentially develop novel therapeutic targets.

## Limitations of the study

Our research, while contributing valuable insights, is subject to certain limitations. The mechanisms underlying MMP9's subcellular localization and secretion present complex pathways that require further elucidation, particularly regarding how MMP9's secretory signals are modified during its subcellular journey. Our observations noted distinct MMP9 expression levels in mitochondrial and nuclear fractions between PMA-treated MMP9-overexpressing cells and solely MMP9-overexpressing cells, with no observed disparity in

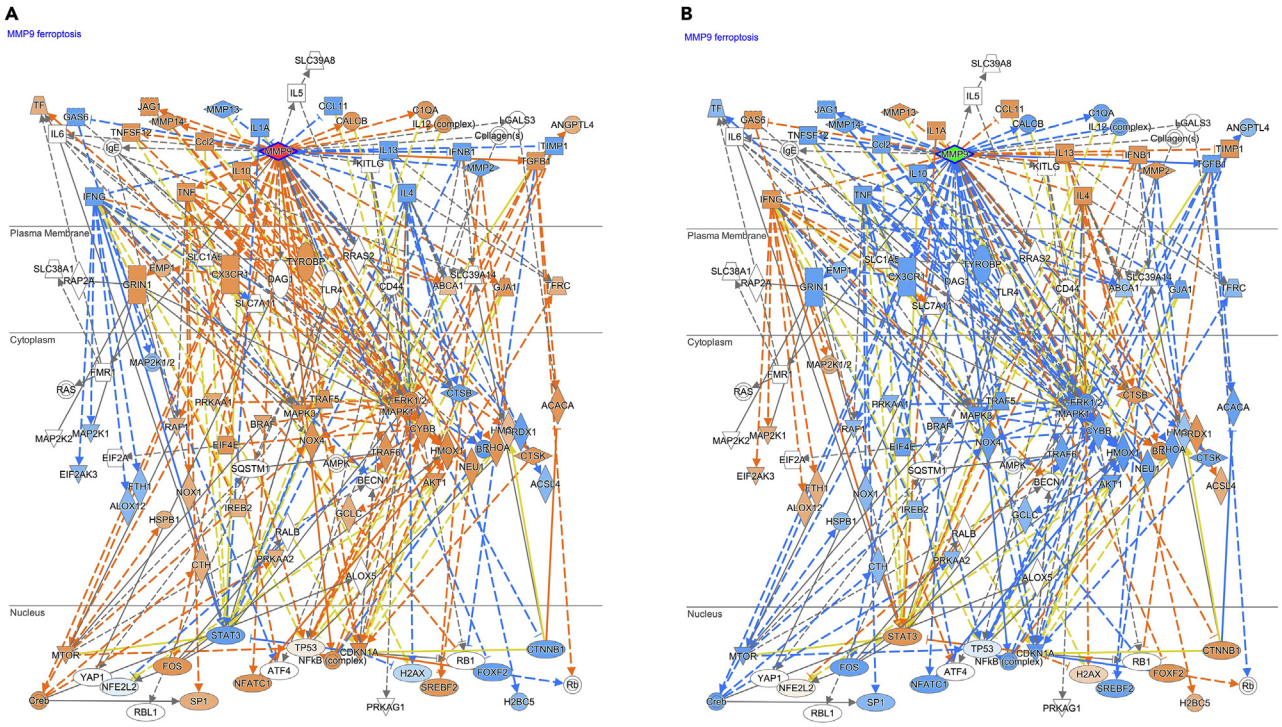


**Figure 6. MMP9's dualistic modulation of the ferroptosis signaling network**

A detailed computational integrated pathway analysis (IPA) elucidating MMP9's involvement in ferroptosis regulation. Through the IPA, we identify the following: (A) Activation dynamics: the illustration captures the cascade of events triggered by MMP9 activation, underscoring its stimulatory effects on various ferroptosis signaling molecules and pathways. The depiction serves to map the enhancement or regulation of ferroptosis by MMP9, offering a pathway-centric view of its promotive actions.

(B) Inhibitory dynamics: the analysis shifts focus to the suppression landscape, dissecting the effects of MMP9 inhibition. This part details the intricate impact on ferroptosis circuitry and the consequent therapeutic angles, emphasizing MMP9 as a manipulable node within this cell death paradigm. By bifurcating MMP9's influence on ferroptosis into activation and inhibition, the analysis furnishes a comprehensive perspective of its ambivalent regulatory capacity. These insights cement MMP9's stature as a strategic molecular target for therapeutic strategies aimed at diseases implicated in ferroptotic processes.

the cytosolic fraction. This could be due to PMA's influence on MMP9 expression via the nuclear factor κB (NF-κB)-dependent pathway.[26] Additionally, intracellular MMP9 may influence epigenetic landscapes through DNA methylation,[30] indicating a significant nuclear role for MMP9. The extent to which these processes elevate nuclear MMP9 expression in PMA-treated cells warrants additional investigation.

While our findings indicate that MMP9 suppresses the transcription factors SP1, NRF2, CREB, ATF4, and FOXO3, pivotal for GPX4 regulation, the specific mechanism behind this effect is yet to be fully understood. PLA results lend support to the hypothesis that MMP9 closely interacts with these transcription factors, hinting at a significant modulatory role essential for controlling GPX4 expression. These insights lay a foundational basis for future investigations into MMP9's regulatory influence over these key transcription factors.

Our LC-MS/MS analysis post-immunoprecipitation did not reveal direct protein-protein interactions between MMP9 and the transcription factors that govern GPX4. This could be due to technical limitations of LC-MS/MS or due to indirect effects of MMP9 on these transcription factors. Further, our IPA (Figure 6) unveils a spectrum of pathways, both direct and indirect, that MMP9 could modulate. These insights underscore a critical avenue for future research to dissect the nuanced roles of MMP9 in regulating GPX4, employing more refined or alternative methodologies to elucidate the precise nature of these regulatory interactions.

Autophagy plays a pivotal role in ferroptosis, particularly through ferritinophagy enhancing ferrous iron levels, and reactive oxygen species (ROS) are crucial for lipid peroxidation in ferroptosis.[4] Given MMP9's involvement in both autophagy and ROS regulation,[29,30] further research is necessary to understand MMP9's influence on these processes in ferroptosis control.

Our current findings are based on *in vitro* studies, highlighting the need for *in vivo* validation to elucidate MMP9's roles across different cellular and tissue contexts. Future work involving MMP9 knockout and transgenic animal models will provide deeper insights into MMP9's tissue-specific functions.

Lastly, our research utilized healthy cell models to isolate MMP9 signaling effects on ferroptosis from pathology-specific influences. However, to enhance clinical relevance, forthcoming studies should incorporate disease models where ferroptosis is implicated, ensuring the broader applicability of our findings.

## STAR★METHODS

Detailed methods are provided in the online version of this paper and include the following:

- KEY RESOURCES TABLE
- RESOURCE AVAILABILITY
  - Lead contact
  - Materials availability
  - Data and code availability
- EXPERIMENTAL MODEL AND STUDY PARTICIPANT DETAILS
  - Cell line
- METHOD DETAILS
  - Cell culture
  - Cell fractionation
  - Cytotoxicity assay
  - Western blotting
  - Co-immunoprecipitation
  - Proximal ligation assay (PLA)
  - In-silico protein-protein interaction
  - Ingenuity pathway analysis (IPA)
  - Confocal microscopy
  - MMP9 and mutant MMP9 expression vectors
  - Liquid chromatography with tandem mass spectrometry (LC-MS/MS) analysis
- QUANTIFICATION AND STATISTICAL ANALYSIS

## SUPPLEMENTAL INFORMATION

Supplemental information can be found online at https://doi.org/10.1016/j.isci.2024.110622.

## ACKNOWLEDGMENTS

This research was supported, in part, by the National Institutes of Health (NIH) grant R56HL156806, the National Institute on Alcohol Abuse and Alcoholism grant 1P50AA030407, and the University of Nebraska Collaboration Initiative grants to P.K.M. and the American Heart Association Predoctoral Fellowship 24PRE1181407 to F.I.G.

## AUTHOR CONTRIBUTIONS

P.K.M. and F.I.G. conceptualized the study. F.I.G. conducted the experiments. P.K.M. wrote the manuscript. Both F.I.G. and P.K.M. approved the final manuscript.

## DECLARATION OF INTERESTS

The authors declare no competing interests.

Received: December 12, 2023
Revised: February 8, 2024
Accepted: July 26, 2024
Published: July 30, 2024

## REFERENCES

1. Dixon, S.J., Lemberg, K.M., Lamprecht, M.R., Skouta, R., Zaitsev, E.M., Gleason, C.E., Patel, D.N., Bauer, A.J., Cantley, A.M., Yang, W.S., et al. (2012). Ferroptosis: an iron-dependent form of nonapoptotic cell death. Cell *149*, 1060–1072. https://doi.org/10.1016/j.cell.2012.03.042.
2. Stockwell, B.R. (2022). Ferroptosis turns 10: Emerging mechanisms, physiological functions, and therapeutic applications. Cell *185*, 2401–2421. https://doi.org/10.1016/j.cell.2022.06.003.
3. Gawargi, F.I., and Mishra, P.K. (2024). Regulation of cardiac ferroptosis in diabetic human heart failure: uncovering molecular pathways and key targets. Cell Death Discov. *10*, 268. https://doi.org/10.1038/s41420-024-02044-w.
4. Gawargi, F.I., and Mishra, P.K. (2023). Ironing out the details: ferroptosis and its relevance to diabetic cardiomyopathy. Am. J. Physiol. Regul. Integr. Comp. Physiol. *325*, R665–R681. https://doi.org/10.1152/ajpregu.00117.2023.
5. Mishra, P.K., Adameova, A., Hill, J.A., Baines, C.P., Kang, P.M., Downey, J.M., Narula, J., Takahashi, M., Abbate, A., Piristine, H.C., et al. (2019). Guidelines for evaluating myocardial cell death. Am. J. Physiol. Heart Circ. Physiol. *317*, H891–H922. https://doi.org/10.1152/ajpheart.00259.2019.
6. Kim, J.S., Kwon, W.Y., Suh, G.J., Kim, K.S., Jung, Y.S., Kim, S.H., and Lee, S.E. (2016). Plasma glutathione reductase activity and prognosis of septic shock. J. Surg. Res. *200*, 298–307. https://doi.org/10.1016/j.jss.2015.07.044.
7. Alim, I., Caulfield, J.T., Chen, Y., Swarup, V., Geschwind, D.H., Ivanova, E., Seravalli, J., Ai, Y., Sansing, L.H., Ste Marie, E.J., et al. (2019). Selenium Drives a Transcriptional

Adaptive Program to Block Ferroptosis and Treat Stroke. Cell *177*, 1262–1279.e25. https://doi.org/10.1016/j.cell.2019.03.032.

8. Wang, Z., Zhang, X., Tian, X., Yang, Y., Ma, L., Wang, J., and Yu, Y. (2021). CREB stimulates GPX4 transcription to inhibit ferroptosis in lung adenocarcinoma. Oncol. Rep. *45*, 88. https://doi.org/10.3892/or.2021.8039.
9. Zhao, C., Sun, G., Li, Y., Kong, K., Li, X., Kan, T., Yang, F., Wang, L., and Wang, X. (2023). Forkhead box O3 attenuates osteoarthritis by suppressing ferroptosis through inactivation of NF-kappaB/MAPK signaling. J. Orthop. Translat. *39*, 147–162. https://doi.org/10.1016/j.jot.2023.02.005.
10. Mukherjee, D., Chakraborty, S., Bercz, L., D'Alesio, L., Wedig, J., Torok, M.A., Pfau, T., Lathrop, H., Jasani, S., Guenther, A., et al. (2023). Tomatidine targets ATF4-dependent signaling and induces ferroptosis to limit pancreatic cancer progression. iScience *26*, 107408. https://doi.org/10.1016/j.isci.2023.107408.
11. Chen, D., Fan, Z., Rauh, M., Buchfelder, M., Eyupoglu, I.Y., and Savaskan, N. (2017). ATF4 promotes angiogenesis and neuronal cell death and confers ferroptosis in a xCT-dependent manner. Oncogene *36*, 5593–5608. https://doi.org/10.1038/onc.2017.146.
12. Wang, Y., Yan, S., Liu, X., Deng, F., Wang, P., Yang, L., Hu, L., Huang, K., and He, J. (2022). PRMT4 promotes ferroptosis to aggravate doxorubicin-induced cardiomyopathy via inhibition of the Nrf2/GPX4 pathway. Cell Death Differ. *29*, 1982–1995. https://doi.org/10.1038/s41418-022-00990-5.
13. Handy, D.E., and Loscalzo, J. (2022). The role of glutathione peroxidase-1 in health and disease. Free Radic. Biol. Med. *188*, 146–161. https://doi.org/10.1016/j.freeradbiomed.2022.06.004.
14. Doll, S., Freitas, F.P., Shah, R., Aldrovandi, M., da Silva, M.C., Ingold, I., Goya Grocin, A., Xavier da Silva, T.N., Panzilius, E., Scheel, C.H., et al. (2019). FSP1 is a glutathione-independent ferroptosis suppressor. Nature *575*, 693–698. https://doi.org/10.1038/s41586-019-1707-0.
15. Liao, S., Huang, M., Liao, Y., and Yuan, C. (2023). HMOX1 Promotes Ferroptosis Induced by Erastin in Lens Epithelial Cell through Modulates Fe(2+) Production. Curr. Eye Res. *48*, 25–33. https://doi.org/10.1080/02713683.2022.2138450.
16. Donovan, A., Lima, C.A., Pinkus, J.L., Pinkus, G.S., Zon, L.I., Robine, S., and Andrews, N.C. (2005). The iron exporter ferroportin/Slc40a1 is essential for iron homeostasis. Cell Metab. *1*, 191–200. https://doi.org/10.1016/j.cmet.2005.01.003.
17. Zarjou, A., Bolisetty, S., Joseph, R., Traylor, A., Apostolov, E.O., Arosio, P., Balla, J., Verlander, J., Darshan, D., Kuhn, L.C., and Agarwal, A. (2013). Proximal tubule H-ferritin mediates iron trafficking in acute kidney injury. J. Clin. Invest. *123*, 4423–4434. https://doi.org/10.1172/JCI67867.
18. Wang, Y., Qiu, S., Wang, H., Cui, J., Tian, X., Miao, Y., Zhang, C., Cao, L., Ma, L., Xu, X., et al. (2021). Transcriptional Repression of Ferritin Light Chain Increases Ferroptosis Sensitivity in Lung Adenocarcinoma. Front. Cell Dev. Biol. *9*, 719187. https://doi.org/10.3389/fcell.2021.719187.
19. Ryu, M.S., Duck, K.A., and Philpott, C.C. (2018). Ferritin iron regulators, PCBP1 and NCOA4, respond to cellular iron status in developing red cells. Blood Cells Mol. Dis. *69*, 75–81. https://doi.org/10.1016/j.bcmd.2017.09.009.
20. Wang, X., Chen, X., Zhou, W., Men, H., Bao, T., Sun, Y., Wang, Q., Tan, Y., Keller, B.B., Tong, Q., et al. (2022). Ferroptosis is essential for diabetic cardiomyopathy and is prevented by sulforaphane via AMPK/NRF2 pathways. Acta Pharm. Sin. B *12*, 708–722. https://doi.org/10.1016/j.apsb.2021.10.005.
21. Tian, H., Xiong, Y., Zhang, Y., Leng, Y., Tao, J., Li, L., Qiu, Z., and Xia, Z. (2021). Activation of NRF2/FPN1 pathway attenuates myocardial ischemia-reperfusion injury in diabetic rats by regulating iron homeostasis and ferroptosis. Cell Stress Chaperones *27*, 149–164. https://doi.org/10.1007/s12192-022-01257-1.
22. Liu, Y., Lu, S., Wu, L.L., Yang, L., Yang, L., and Wang, J. (2023). The diversified role of mitochondria in ferroptosis in cancer. Cell Death Dis. *14*, 519. https://doi.org/10.1038/s41419-023-06045-y.
23. Wang, Y.Q., Chang, S.Y., Wu, Q., Gou, Y.J., Jia, L., Cui, Y.M., Yu, P., Shi, Z.H., Wu, W.S., Gao, G., and Chang, Y.Z. (2016). The Protective Role of Mitochondrial Ferritin on Erastin-Induced Ferroptosis. Front. Aging Neurosci. *8*, 308. https://doi.org/10.3389/fnagi.2016.00308.
24. Fields, G.B. (2019). The Rebirth of Matrix Metalloproteinase Inhibitors: Moving Beyond the Dogma. Cells *8*, 984. https://doi.org/10.3390/cells8090984.
25. Choi, J.H., Han, E.H., Hwang, Y.P., Choi, J.M., Choi, C.Y., Chung, Y.C., Seo, J.K., and Jeong, H.G. (2010). Suppression of PMA-induced tumor cell invasion and metastasis by aqueous extract isolated from Prunella vulgaris via the inhibition of NF-kappaB-dependent MMP-9 expression. Food Chem. Toxicol. *48*, 564–571. https://doi.org/10.1016/j.fct.2009.11.033.
26. Shin, Y., Yoon, S.H., Choe, E.Y., Cho, S.H., Woo, C.H., Rho, J.Y., and Kim, J.H. (2007). PMA-induced up-regulation of MMP-9 is regulated by a PKCalpha-NF-kappaB cascade in human lung epithelial cells. Exp. Mol. Med. *39*, 97–105. https://doi.org/10.1038/emm.2007.11.
27. Rybakowski, J.K. (2009). Matrix Metalloproteinase-9 (MMP9)-A Mediating Enzyme in Cardiovascular Disease, Cancer, and Neuropsychiatric Disorders. Cardiovasc. Psychiatry Neurol. *2009*, 904836. https://doi.org/10.1155/2009/904836.
28. Yabluchanskiy, A., Ma, Y., Iyer, R.P., Hall, M.E., and Lindsey, M.L. (2013). Matrix metalloproteinase-9: Many shades of function in cardiovascular disease. Physiology *28*, 391–403. https://doi.org/10.1152/physiol.00029.2013.
29. Yadav, S.K., Kambis, T.N., Kar, S., Park, S.Y., and Mishra, P.K. (2020). MMP9 mediates acute hyperglycemia-induced human cardiac stem cell death by upregulating apoptosis and pyroptosis *in vitro*. Cell Death Dis. *11*, 186. https://doi.org/10.1038/s41419-020-2367-6.
30. Yadav, S.K., and Mishra, P.K. (2021). Intracellular matrix metalloproteinase-9 mediates epigenetic modifications and autophagy to regulate differentiation in human cardiac stem cells. Stem Cell. *39*, 497–506. https://doi.org/10.1002/stem.3330.
31. Bailon, E., Aguilera-Montilla, N., Gutierrez-Gonzalez, A., Ugarte-Berzal, E., Van den Steen, P.E., Opdenakker, G., Garcia-Marco, J.A., and Garcia-Pardo, A. (2018). A catalytically inactive gelatinase B/MMP-9 mutant impairs homing of chronic lymphocytic leukemia cells by altering migration regulatory pathways. Biochem. Biophys. Res. Commun. *495*, 124–130. https://doi.org/10.1016/j.bbrc.2017.10.129.
32. Gawargi, F.I., and Mishra, P.K. (2024). Deciphering MMP9's dual role in regulating SOD3 through protein-protein interactions. Can. J. Physiol. Pharmacol. *102*, 196–205. https://doi.org/10.1139/cjpp-2023-0256.
33. Egorov, D., Kopaliani, I., Ameln, A.K.v., Speier, S., and Deussen, A. (2024). Mechanism of pro-MMP9 activation in co-culture of pro-inflammatory macrophages and cardiomyocytes. Exp. Cell Res. *434*, 113868. https://doi.org/10.1016/j.yexcr.2023.113868.
34. Gawargi, F.I., and Mishra, P.K. (2024). Deciphering MMP9's Dual Role in Regulating SOD3 through Protein-Protein Interaction. Can. J. Physiol. Pharmacol. *102*, 196–205. https://doi.org/10.1139/cjpp-2023-0256.
35. Tan, E., Chin, C.S.H., Lim, Z.F.S., and Ng, S.K. (2021). HEK293 Cell Line as a Platform to Produce Recombinant Proteins and Viral Vectors. Front. Bioeng. Biotechnol. *9*, 796991. https://doi.org/10.3389/fbioe.2021.796991.
36. Liu, W., Ostberg, N., Yalcinkaya, M., Dou, H., Endo-Umeda, K., Tang, Y., Hou, X., Xiao, T., Fidler, T.P., Abramowicz, S., et al. (2022). Erythroid lineage Jak2V617F expression promotes atherosclerosis through erythrophagocytosis and macrophage ferroptosis. J. Clin. Invest. *132*, e155724. https://doi.org/10.1172/JCI155724.
37. Zhu, Y., Yang, X., Zhou, J., Chen, L., Zuo, P., Chen, L., Jiang, L., Li, T., Wang, D., Xu, Y., et al. (2022). miR-340-5p Mediates Cardiomyocyte Oxidative Stress in Diabetes-Induced Cardiac Dysfunction by Targeting Mcl-1. Oxid. Med. Cell. Longev. *2022*, 3182931. https://doi.org/10.1155/2022/3182931.
38. Chai, Y.C., Ashraf, S.S., Rokutan, K., Johnston, R.B., Jr., and Thomas, J.A. (1994). S-thiolation of individual human neutrophil proteins including actin by stimulation of the respiratory burst: evidence against a role for glutathione disulfide. Arch. Biochem. Biophys. *310*, 273–281. https://doi.org/10.1006/abbi.1994.1167.
39. Zitka, O., Skalickova, S., Gumulec, J., Masarik, M., Adam, V., Hubalek, J., Trnkova, L., Kruseova, J., Eckschlager, T., and Kizek, R. (2012). Redox status expressed as GSH:GSSG ratio as a marker for oxidative stress in paediatric tumour patients. Oncol. Lett. *4*, 1247–1253. https://doi.org/10.3892/ol.2012.931.
40. Xie, D., Chen, F., Zhang, Y., Shi, B., Song, J., Chaudhari, K., Yang, S.H., Zhang, G.J., Sun, X., Taylor, H.S., et al. (2022). Let-7 underlies metformin-induced inhibition of hepatic glucose production. Proc. Natl. Acad. Sci. USA *119*, e2122217119. https://doi.org/10.1073/pnas.2122217119.
41. Kambis, T.N., Tofilau, H.M.N., Gawargi, F.I., Chandra, S., and Mishra, P.K. (2021). Regulating Polyamine Metabolism by miRNAs in Diabetic Cardiomyopathy. Curr. Diab. Rep. *21*, 52. https://doi.org/10.1007/s11892-021-01429-w.
42. Alam, M.S. (2018). Proximity Ligation Assay (PLA). Curr. Protoc. Immunol. *123*, e58. https://doi.org/10.1002/cpim.58.

43. Xie, Y., Kang, R., Klionsky, D.J., and Tang, D. (2023). GPX4 in cell death, autophagy, and disease. Autophagy *19*, 2621–2638. https://doi.org/10.1080/15548627.2023.2218764.
44. Bersuker, K., Hendricks, J.M., Li, Z., Magtanong, L., Ford, B., Tang, P.H., Roberts, M.A., Tong, B., Maimone, T.J., Zoncu, R., et al. (2019). The CoQ oxidoreductase FSP1 acts parallel to GPX4 to inhibit ferroptosis. Nature *575*, 688–692. https://doi.org/10.1038/s41586-019-1705-2.
45. Meng, Z., Liang, H., Zhao, J., Gao, J., Liu, C., Ma, X., Liu, J., Liang, B., Jiao, X., Cao, J., and Wang, Y. (2021). HMOX1 upregulation promotes ferroptosis in diabetic atherosclerosis. Life Sci. *284*, 119935. https://doi.org/10.1016/j.lfs.2021.119935.
46. Protchenko, O., Baratz, E., Jadhav, S., Li, F., Shakoury-Elizeh, M., Gavrilova, O., Ghosh, M.C., Cox, J.E., Maschek, J.A., Tyurin, V.A., et al. (2021). Iron Chaperone Poly rC Binding Protein 1 Protects Mouse Liver From Lipid Peroxidation and Steatosis. Hepatology *73*, 1176–1193. https://doi.org/10.1002/hep.31328.
47. Shen, L., Zhang, J., Zheng, Z., Yang, F., Liu, S., Wu, Y., Chen, Y., Xu, T., Mao, S., Yan, Y., et al. (2022). PHGDH Inhibits Ferroptosis and Promotes Malignant Progression by Upregulating SLC7A11 in Bladder Cancer. Int. J. Biol. Sci. *18*, 5459–5474. https://doi.org/10.7150/ijbs.74546.
48. Zhao, Y., Ruan, X., Cheng, J., Xu, X., Gu, M., and Mueck, A.O. (2023). PGRMC1 promotes triple-negative breast cancer cell growth via suppressing ferroptosis. Climacteric *26*, 135–142. https://doi.org/10.1080/13697137.2023.2170225.
49. Sun, J., Zhou, C., Zhao, Y., Zhang, X., Chen, W., Zhou, Q., Hu, B., Gao, D., Raatz, L., Wang, Z., et al. (2021). Quiescin sulfhydryl oxidase 1 promotes sorafenib-induced ferroptosis in hepatocellular carcinoma by driving EGFR endosomal trafficking and inhibiting NRF2 activation. Redox Biol. *41*, 101942. https://doi.org/10.1016/j.redox.2021.101942.
50. Wang, Z., Li, R., Hou, N., Zhang, J., Wang, T., Fan, P., Ji, C., Zhang, B., Liu, L., Wang, Y., et al. (2023). PRMT5 reduces immunotherapy efficacy in triple-negative breast cancer by methylating KEAP1 and inhibiting ferroptosis. J. Immunother. Cancer *11*, e006890. https://doi.org/10.1136/jitc-2023-006890.
51. Shi, Z., Zhang, H., Shen, Y., Zhang, S., Zhang, X., Xu, Y., and Sun, D. (2023). SETD1A-mediated H3K4me3 methylation upregulates lncRNA HOXC-AS3 and the binding of HOXC-AS3 to EP300 and increases EP300 stability to suppress the ferroptosis of NSCLC cells. Thorac Cancer *14*, 2579–2590. https://doi.org/10.1111/1759-7714.15037.
52. Li, Y., Li, J., Li, Z., Wei, M., Zhao, H., Miyagishi, M., Wu, S., and Kasim, V. (2022). Homeostasis Imbalance of YY2 and YY1 Promotes Tumor Growth by Manipulating Ferroptosis. Adv. Sci. *9*, e2104836. https://doi.org/10.1002/advs.202104836.
53. Yang, W., Mu, B., You, J., Tian, C., Bin, H., Xu, Z., Zhang, L., Ma, R., Wu, M., Zhang, G., et al. (2022). Non-classical ferroptosis inhibition by a small molecule targeting PHB2. Nat. Commun. *13*, 7473. https://doi.org/10.1038/s41467-022-35294-2.
54. Lu, J., Xu, S., Huo, Y., Sun, D., Hu, Y., Wang, J., Zhang, X., Wang, P., Li, Z., Liang, M., et al. (2021). Sorting nexin 3 induces heart failure via promoting retromer-dependent nuclear trafficking of STAT3. Cell Death Differ. *28*, 2871–2887. https://doi.org/10.1038/s41418-021-00789-w.
55. Schmitt, A., Grimm, M., Kreienkamp, N., Junge, H., Labisch, J., Schuhknecht, L., Schönfeld, C., Görsch, E., Tibello, A., Menck, K., et al. (2023). BRD4 inhibition sensitizes diffuse large B-cell lymphoma cells to ferroptosis. Blood *142*, 1143–1155. https://doi.org/10.1182/blood.2022019274.
56. Jiang, B., Zhao, Y.Q., Shi, M., Song, L., Wang, Q., Qin, Q.M., Song, X.M., Wu, S., Fang, Z., and Liu, X.Y. (2020). DNAJB6 Promotes Ferroptosis in Esophageal Squamous Cell Carcinoma. Dig. Dis. Sci. *65*, 1999–2008. https://doi.org/10.1007/s10620-019-05929-4.
57. Hassannia, B., Vandenabeele, P., and Vanden Berghe, T. (2019). Targeting Ferroptosis to Iron Out Cancer. Cancer Cell *35*, 830–849. https://doi.org/10.1016/j.ccell.2019.04.002.
58. Wang, T.X., Liang, J.Y., Zhang, C., Xiong, Y., Guan, K.L., and Yuan, H.X. (2019). The oncometabolite 2-hydroxyglutarate produced by mutant IDH1 sensitizes cells to ferroptosis. Cell Death Dis. *10*, 755. https://doi.org/10.1038/s41419-019-1984-4.
59. Chen, X., Kang, R., Kroemer, G., and Tang, D. (2021). Organelle-specific regulation of ferroptosis. Cell Death Differ. *28*, 2843–2856. https://doi.org/10.1038/s41418-021-00859-z.
60. Li, D., Wang, Y., Dong, C., Chen, T., Dong, A., Ren, J., Li, W., Shu, G., Yang, J., Shen, W., et al. (2023). CST1 inhibits ferroptosis and promotes gastric cancer metastasis by regulating GPX4 protein stability via OTUB1. Oncogene *42*, 83–98. https://doi.org/10.1038/s41388-022-02537-x.
61. Tang, D., Chen, X., Kang, R., and Kroemer, G. (2021). Ferroptosis: molecular mechanisms and health implications. Cell Res. *31*, 107–125. https://doi.org/10.1038/s41422-020-00441-1.
62. Zhang, L.-L., Tang, R.-J., and Yang, Y.-J. (2022). The underlying pathological mechanism of ferroptosis in the development of cardiovascular disease. Front. Cardiovasc. Med. *9*, 964034. https://doi.org/10.3389/fcvm.2022.964034.
63. Ouyang, X., Zhu, R., Lin, L., Wang, X., Zhuang, Q., and Hu, D. (2023). GAPDH Is a Novel Ferroptosis-Related Marker and Correlates with Immune Microenvironment in Lung Adenocarcinoma. Metabolites *13*, 142. https://doi.org/10.3390/metabo13020142.
64. Jiang, L., Kon, N., Li, T., Wang, S.-J., Su, T., Hibshoosh, H., Baer, R., and Gu, W. (2015). Ferroptosis as a p53-mediated activity during tumour suppression. Nature *520*, 57–62. https://doi.org/10.1038/nature14344.
65. Tao, Q., Qiu, X., Li, C., Zhou, J., Gu, L., Zhang, L., Pang, J., Zhang, L., Yin, S., Jiang, Y., and Peng, J. (2022). S100A8 regulates autophagy-dependent ferroptosis in microglia after experimental subarachnoid hemorrhage. Exp. Neurol. *357*, 114171. https://doi.org/10.1016/j.expneurol.2022.114171.
66. Cui, J., Ma, Q., Zhang, C., Li, Y., Liu, J., Xie, K., Luo, E., Zhai, M., and Tang, C. (2023). Keratin 18 Depletion as a Possible Mechanism for the Induction of Apoptosis and Ferroptosis in the Rat Hippocampus After Hypobaric Hypoxia. Neuroscience *513*, 64–75. https://doi.org/10.1016/j.neuroscience.2022.11.009.
67. Zeng, K., Li, W., Wang, Y., Zhang, Z., Zhang, L., Zhang, W., Xing, Y., and Zhou, C. (2023). Inhibition of CDK1 Overcomes Oxaliplatin Resistance by Regulating ACSL4-mediated Ferroptosis in Colorectal Cancer. Adv. Sci. *10*, e2301088.
68. Zhang, T., Sun, L., Hao, Y., Suo, C., Shen, S., Wei, H., Ma, W., Zhang, P., Wang, T., Gu, X., et al. (2022). ENO1 suppresses cancer cell ferroptosis by degrading the mRNA of iron regulatory protein 1. Nat. Cancer *3*, 75–89. https://doi.org/10.1038/s43018-021-00299-1.
69. Wu, F., Xiong, G., Chen, Z., Lei, C., Liu, Q., and Bai, Y. (2022). SLC3A2 inhibits ferroptosis in laryngeal carcinoma via mTOR pathway. Hereditas *159*, 6. https://doi.org/10.1186/s41065-022-00225-0.
70. Berr, A.L., Wiese, K., Dos Santos, G., Koch, C.M., Anekalla, K.R., Kidd, M., Davis, J.M., Cheng, Y., Hu, Y.-S., and Ridge, K.M. (2023). Vimentin is required for tumor progression and metastasis in a mouse model of non-small cell lung cancer. Oncogene *42*, 2074–2087. https://doi.org/10.1038/s41388-023-02703-9.
71. Tan, X., Huang, X., Niu, B., Guo, X., Lei, X., and Qu, B. (2022). Targeting GSTP1-dependent ferroptosis in lung cancer radiotherapy: Existing evidence and future directions. Front. Mol. Biosci. *9*, 1102158. https://doi.org/10.3389/fmolb.2022.1102158. eCollection 2022.
72. Hong, T., Lei, G., Chen, X., Li, H., Zhang, X., Wu, N., Zhao, Y., Zhang, Y., and Wang, J. (2021). PARP inhibition promotes ferroptosis via repressing SLC7A11 and synergizes with ferroptosis inducers in BRCA-proficient ovarian cancer. Redox Biol. *42*, 101928. https://doi.org/10.1016/j.redox.2021.101928.
73. Bai, L., Yan, F., Deng, R., Gu, R., Zhang, X., and Bai, J. (2021). Thioredoxin-1 Rescues $MPP^+$/MPTP-Induced Ferroptosis by Increasing Glutathione Peroxidase 4. Mol. Neurobiol. *58*, 3187–3197. https://doi.org/10.1007/s12035-021-02320-1.
74. Wu, K., Yan, M., Liu, T., Wang, Z., Duan, Y., Xia, Y., Ji, G., Shen, Y., Wang, L., Li, L., et al. (2023). Creatine kinase B suppresses ferroptosis by phosphorylating GPX4 through a moonlighting function. Nat. Cell Biol. *25*, 714–725. https://doi.org/10.1038/s41556-023-01133-9.
75. Kang, L., Wang, D., Shen, T., Liu, X., Dai, B., Zhou, D., Shen, H., Gong, J., Li, G., Hu, Y., et al. (2023). PDIA4 confers resistance to ferroptosis via induction of ATF4/SLC7A11 in renal cell carcinoma. Cell Death Dis. *14*, 193.
76. Zhou, R., Qiu, L., Zhou, L., Geng, R., Yang, S., and Wu, J. (2023). P4HA1 activates HMGCS1 to promote nasopharyngeal carcinoma ferroptosis resistance and progression. Cell. Signal. *105*, 110609. https://doi.org/10.1016/j.cellsig.2023.110609.
77. Zhang, H., Zhu, S., Zhou, H., Li, R., Xia, X., and Xiong, H. (2023). Identification of MTHFD2 as a prognostic biomarker and ferroptosis regulator in triple-negative breast cancer. Front. Oncol. *13*, 1098357. https://doi.org/10.3389/fonc.2023.1098357.
78. Cai, H., Ren, Y., Chen, S., Wang, Y., and Chu, L. (2023). Ferroptosis and tumor immunotherapy: A promising combination therapy for tumors. Front. Oncol. *13*,

1119369. https://doi.org/10.3389/fonc.2023.1119369.
79. Dang, Q., Sun, Z., Wang, Y., Wang, L., Liu, Z., and Han, X. (2022). Ferroptosis: a double-edged sword mediating immune tolerance of cancer. Cell Death Dis. *13*, 925. https://doi.org/10.1038/s41419-022-05384-6.
80. Zhang, J., Li, Y., Zou, J., Lai, C.-T., Zeng, T., Peng, J., Zou, W.-D., Cao, B., Liu, D., Zhu, L.-Y., et al. (2022). Comprehensive analysis of the glutathione S-transferase Mu (GSTM) gene family in ovarian cancer identifies prognostic and expression significance. Front. Oncol. *12*, 968547. https://doi.org/10.3389/fonc.2022.968547.
81. Wu, H., Wang, F., Ta, N., Zhang, T., and Gao, W. (2021). The Multifaceted Regulation of Mitochondria in Ferroptosis. Life (Basel) *11*, 222. https://doi.org/10.3390/life11030222.
82. Wang, X., Wang, Y., Li, Z., Qin, J., and Wang, P. (2021). Regulation of Ferroptosis Pathway by Ubiquitination. Front. Cell Dev. Biol. *9*, 699304. https://doi.org/10.3389/fcell.2021.699304.
83. Zhan, Y., Yang, Z., Zhan, F., Huang, Y., and Lin, S. (2023). SIRT1 is transcriptionally repressed by YY1 and suppresses ferroptosis in rheumatoid arthritis. Adv. Rheumatol. *63*, 9. https://doi.org/10.1186/s42358-023-00289-0.
84. Yang, H., Sun, W., Bi, T., Wang, Q., Wang, W., Xu, Y., Liu, Z., and Li, J. (2023). The PTBP1-NCOA4 axis promotes ferroptosis in liver cancer cells. Oncol. Rep. *49*, 45. https://doi.org/10.3892/or.2023.8482.
85. Song, Q., Peng, S., Che, F., and Zhu, X. (2022). Artesunate induces ferroptosis via modulation of p38 and ERK signaling pathway in glioblastoma cells. J. Pharmacol. Sci. *148*, 300–306. https://doi.org/10.1016/j.jphs.2022.01.007.
86. Lu, B., Chen, X.-B., Hong, Y.-C., Zhu, H., He, Q.-J., Yang, B., Ying, M.-D., and Cao, J. (2019). Identification of PRDX6 as a regulator of ferroptosis. Acta Pharmacol. Sin. *40*, 1334–1342. https://doi.org/10.1038/s41401-019-0233-9.
87. Ma, M., Kong, P., Huang, Y., Wang, J., Liu, X., Hu, Y.R., Chen, X., Du, C., and Yang, H. (2022). Activation of MAT2A-ACSL3 pathway protects cells from ferroptosis in gastric cancer. Free Radic. Biol. Med. *181*, 288–299. https://doi.org/10.1016/j.freeradbiomed.2022.02.015.
88. Chen, Y., Li, S., Yin, M., Li, Y., Chen, C., Zhang, J., Sun, K., Kong, X., Chen, Z., and Qian, J. (2023). Isorhapontigenin Attenuates Cardiac Microvascular Injury in Diabetes via the Inhibition of Mitochondria-Associated Ferroptosis Through PRDX2-MFN2-ACSL4 Pathways. Diabetes *72*, 389–404. https://doi.org/10.2337/db22-0553.
89. Minami, J.K., Morrow, D., Bayley, N.A., Fernandez, E.G., Salinas, J.J., Tse, C., Zhu, H., Su, B., Plawat, R., Jones, A., et al. (2023). CDKN2A deletion remodels lipid metabolism to prime glioblastoma for ferroptosis. Cancer Cell *41*, 1048–1060.e9. https://doi.org/10.1016/j.ccell.2023.05.001.
90. Yang, Y., Luo, M., Zhang, K., Zhang, J., Gao, T., Connell, D.O., Yao, F., Mu, C., Cai, B., Shang, Y., and Chen, W. (2020). Nedd4 ubiquitylates VDAC2/3 to suppress erastin-induced ferroptosis in melanoma. Nat. Commun. *11*, 433. https://doi.org/10.1038/s41467-020-14324-x.
91. Murari, A., Goparaju, N.S.V., Rhooms, S.-K., Hossain, K.F.B., Liang, F.G., Garcia, C.J., Osei, C., Liu, T., Li, H., Kitsis, R.N., et al. (2022). IDH2-mediated regulation of the biogenesis of the oxidative phosphorylation system. Sci. Adv. *8*, eabl8716. https://doi.org/10.1126/sciadv.abl8716.
92. Li, Y., Yang, W., Zheng, Y., Dai, W., Ji, J., Wu, L., Cheng, Z., Zhang, J., Li, J., Xu, X., et al. (2023). Targeting fatty acid synthase modulates sensitivity of hepatocellular carcinoma to sorafenib via ferroptosis. J. Exp. Clin. Cancer Res. *42*, 6.
93. Wang, K., He, J., Tu, C., Xu, H., Zhang, X., Lv, Y., and Song, C. (2022). Upregulation of CCT3 predicts poor prognosis and promotes cell proliferation via inhibition of ferroptosis and activation of AKT signaling in lung adenocarcinoma BMC. Mol. Cell Biol. *23*, 25. https://doi.org/10.1186/s12860-022-00424-7.
94. Chen, Z., Yan, Y., Qi, C., Liu, J., Li, L., and Wang, J. (2021). The Role of Ferroptosis in Cardiovascular Disease and Its Therapeutic Significance. Front. Cardiovasc. Med. *8*, 733229. https://doi.org/10.3389/fcvm.2021.733229.
95. Liu, K., Liu, J., Zou, B., Li, C., Zeh, H.J., Kang, R., Kroemer, G., Huang, J., and Tang, D. (2022). Trypsin-Mediated Sensitization to Ferroptosis Increases the Severity of Pancreatitis in Mice. Cell. Mol. Gastroenterol. Hepatol. *13*, 483–500. https://doi.org/10.1016/j.jcmgh.2021.09.008.
96. Ogor, P., Yoshida, T., Koike, M., and Kakizuka, A. (2021). VCP relocalization limits mitochondrial activity, GSH depletion and ferroptosis during starvation in PC3 prostate cancer cells. Gene Cell. *26*, 570–582. https://doi.org/10.1111/gtc.12872.
97. Nobuta, H., Yang, N., Ng, Y.H., Marro, S.G., Sabeur, K., Chavali, M., Stockley, J.H., Killilea, D.W., Walter, P.B., Zhao, C., et al. (2019). Oligodendrocyte Death in Pelizaeus-Merzbacher Disease Is Rescued by Iron Chelation. Cell Stem Cell *25*, 531–541.e6. https://doi.org/10.1016/j.stem.2019.09.003.
98. Zhang, H., Liu, X., Zhou, L., Deng, Z., and Wang, Y. (2022). Identification of RPS7 as the Biomarker of Ferroptosis in Acute Kidney Injury. BioMed Res. Int. *2022*, 3667339. https://doi.org/10.1155/2022/3667339.
99. Yuan, J., Lv, T., Yang, J., Wu, Z., Yan, L., Yang, J., and Shi, Y. (2022). HDLBP-stabilized lncFAL inhibits ferroptosis vulnerability by diminishing Trim69-dependent FSP1 degradation in hepatocellular carcinoma. Redox Biol. *58*, 102546. https://doi.org/10.1016/j.redox.2022.102546.
100. Ta, N., Qu, C., Wu, H., Zhang, D., Sun, T., Li, Y., Wang, J., Wang, X., Tang, T., Chen, Q., and Liu, L. (2022). Mitochondrial outer membrane protein FUNDC2 promotes ferroptosis and contributes to doxorubicin-induced cardiomyopathy. Proc. Natl. Acad. Sci. USA *119*, e2117396119. https://doi.org/10.1073/pnas.2117396119.
101. Wu, W.-Y., Wang, Z.-X., Li, T.-S., Ding, X.-Q., Liu, Z.-H., Yang, J., Fang, L., and Kong, L.-D. (2022). SSBP1 drives high fructose-induced glomerular podocyte ferroptosis via activating DNA-PK/p53 pathway. Redox Biol. *52*, 102303. https://doi.org/10.1016/j.redox.2022.102303.
102. Guo, T., Zhang, X., Chen, S., Wang, X., and Wang, X. (2024). Targeting lipid biosynthesis on the basis of conventional treatments for clear cell renal cell carcinoma: A promising therapeutic approach. Life Sci. *336*, 122329. https://doi.org/10.1016/j.lfs.2023.122329.
103. Lovatt, M., Adnan, K., Kocaba, V., Dirisamer, M., Peh, G.S.L., and Mehta, J.S. (2020). Peroxiredoxin-1 regulates lipid peroxidation in corneal endothelial cells. Redox Biol. *30*, 101417. https://doi.org/10.1016/j.redox.2019.101417.
104. Luo, P., Liu, D., Zhang, Q., Yang, F., Wong, Y.-K., Xia, F., Zhang, J., Chen, J., Tian, Y., Yang, C., et al. (2022). Celastrol induces ferroptosis in activated HSCs to ameliorate hepatic fibrosis *via* targeting peroxiredoxins and HO-1. Acta Pharm. Sin. B *12*, 2300–2314. https://doi.org/10.1016/j.apsb.2021.12.007.
105. Li, S., Liao, Z., Yin, H., Liu, O., Hua, W., Wu, X., Zhang, Y., Gao, Y., and Yang, C. (2023). G3BP1 coordinates lysophagy activity to protect against compression-induced cell ferroptosis during intervertebral disc degeneration. Cell Prolif. *56*, e13368. https://doi.org/10.1111/cpr.13368.
106. Yuan, F., Sun, Q., Zhang, S., Ye, L., Xu, Y., Deng, G., Xu, Z., Zhang, S., Liu, B., and Chen, Q. (2022). The dual role of p62 in ferroptosis of glioblastoma according to p53 status. Cell Biosci. *12*, 20. https://doi.org/10.1186/s13578-022-00764-z.
107. Lee, J., You, J.H., and Roh, J.-L. (2022). Poly(rC)-binding protein 1 represses ferritinophagy-mediated ferroptosis in head and neck cancer. Redox Biol. *51*, 102276. https://doi.org/10.1016/j.redox.2022.102276.
108. Frey, A.G., Nandal, A., Park, J.H., Smith, P.M., Yabe, T., Ryu, M.-S., Ghosh, M.C., Lee, J., Rouault, T.A., Park, M.H., and Philpott, C.C. (2014). Iron chaperones PCBP1 and PCBP2 mediate the metallation of the dinuclear iron enzyme deoxyhypusine hydroxylase. Proc. Natl. Acad. Sci. USA *111*, 8031–8036. https://doi.org/10.1073/pnas.1402732111.
109. Zhang, Z., Yao, Z., Wang, L., Ding, H., Shao, J., Chen, A., Zhang, F., and Zheng, S. (2018). Activation of ferritinophagy is required for the RNA-binding protein ELAVL1/HuR to regulate ferroptosis in hepatic stellate cells. Autophagy *14*, 2083–2103. https://doi.org/10.1080/15548627.2018.1503146.
110. Morra, F., Merolla, F., Zito Marino, F., Catalano, R., Franco, R., Chieffi, P., and Celetti, A. (2021). The tumour suppressor CCDC6 is involved in ROS tolerance and neoplastic transformation by evading ferroptosis. Heliyon *7*, e08399. https://doi.org/10.1016/j.heliyon.2021.e08399.
111. Chen, X., Zhang, L., He, Y., Huang, S., Chen, S., Zhao, W., and Yu, D. (2023). Regulation of m$^6$A modification on ferroptosis and its potential significance in radiosensitization. Cell Death Discov. *9*, 343.
112. Li, Z., Chen, L., Chen, C., Zhou, Y., Hu, D., Yang, J., Chen, Y., Zhuo, W., Mao, M., Zhang, X., et al. (2020). Targeting ferroptosis in breast cancer. Biomark. Res. *8*, 58. https://doi.org/10.1186/s40364-020-00230-3.
113. He, Z., Yang, J., Sui, C., Zhang, P., Wang, T., Mou, T., Sun, K., Wang, Y., Xu, Z., Li, G., et al. (2022). FAM98A promotes resistance to 5-fluorouracil in colorectal cancer by suppressing ferroptosis. Arch. Biochem. Biophys. *722*, 109216. https://doi.org/10.1016/j.abb.2022.109216.
114. Feng, J., Li, Y., He, F., and Zhang, F. (2023). RBM15 silencing promotes ferroptosis by regulating the TGF-β/Smad2 pathway in lung cancer. Environ. Toxicol. *38*, 950–961. https://doi.org/10.1002/tox.23741.
115. Tang, B., Wang, Y., Zhu, J., Song, J., Fang, S., Weng, Q., Yang, Y., Tu, J., Zhao, Z., Chen,

M., et al. (2023). TACE responser NDRG1 acts as a guardian against ferroptosis to drive tumorgenesis and metastasis in HCC. Biol. Proced. Online *25*, 13. https://doi.org/10.1186/s12575-023-00199-x.

116. Wang, N., Ma, H., Li, J., Meng, C.Y., Zou, J., Wang, H., Liu, K., Liu, M., Xiao, X., Zhang, H., and Wang, K. (2021). HSF1 functions as a key defender against palmitic acid-induced ferroptosis in cardiomyocytes. J. Mol. Cell. Cardiol. *150*, 65–76. https://doi.org/10.1016/j.yjmcc.2020.10.010.
117. Fan, W., Rong, J., Shi, W., Liu, W., Wang, J., Tan, J., Yu, B., and Tong, J. (2023). GATA6 Inhibits Neuronal Autophagy and Ferroptosis in Cerebral ischemia-reperfusion Injury Through a miR-193b/ATG7 axis-dependent Mechanism. Neurochem. Res. *48*, 2552–2567. https://doi.org/10.1007/s11064-023-03918-8.
118. Zhou, W., Zhang, J., Yan, M., Wu, J., Lian, S., Sun, K., Li, B., Ma, J., Xia, J., and Lian, C. (2021). Orlistat induces ferroptosis-like cell death of lung cancer cells. Front. Med. *15*, 922–932. https://doi.org/10.1007/s11684-020-0804-7.
119. Cheng, F., Dou, J., Yang, Y., Sun, S., Chen, R., Zhang, Z., Wei, H., Li, J., and Wu, Z. (2023). Drug-induced lactate confers ferroptosis resistance via p38-SGK1-NEDD4L-dependent upregulation of GPX4 in NSCLC cells. Cell Death Discov. *9*, 165. https://doi.org/10.1038/s41420-023-01463-5.
120. Pan, J., Xiong, W., Zhang, A., Zhang, H., Lin, H., Gao, L., Ke, J., Huang, S., Zhang, J., Gu, J., et al. (2023). The Imbalance of p53-Park7 Signaling Axis Induces Iron Homeostasis Dysfunction in Doxorubicin-Challenged Cardiomyocytes. Adv. Sci. *10*, e2206007. https://doi.org/10.1002/advs.202206007.
121. Mirhadi, S., Zhang, W., Pham, N.-A., Karimzadeh, F., Pintilie, M., Tong, J., Taylor, P., Krieger, J., Pitcher, B., Sykes, J., et al. (2023). Mitochondrial Aconitase ACO2 Links Iron Homeostasis with Tumorigenicity in Non-Small Cell Lung Cancer. Mol. Cancer Res. *21*, 36–50. https://doi.org/10.1158/1541-7786.MCR-22-0163.
122. Jiang, Y., Mao, C., Yang, R., Yan, B., Shi, Y., Liu, X., Lai, W., Liu, Y., Wang, X., Xiao, D., et al. (2017). EGLN1/c-Myc Induced Lymphoid-Specific Helicase Inhibits Ferroptosis through Lipid Metabolic Gene Expression Changes. Theranostics *7*, 3293–3305. https://doi.org/10.7150/thno.19988.
123. Sun, W.-C., Wang, N.-N., Li, R., Sun, X.-C., Liao, J.-W., Yang, G., and Liu, S. (2023). Ferritinophagy activation and sideroflexin1-dependent mitochondrial iron overload contribute to patulin-induced cardiac inflammation and fibrosis. Sci. Total Environ. *892*, 164472. https://doi.org/10.1016/j.scitotenv.2023.164472.
124. Xue, X., Ma, L., Zhang, X., Xu, X., Guo, S., Wang, Y., Qiu, S., Cui, J., Guo, W., Yu, Y., et al. (2022). Tumour cells are sensitised to ferroptosis via RB1CC1-mediated transcriptional reprogramming. Clin. Transl. Med. *12*, e747. https://doi.org/10.1002/ctm2.747.
125. Yuan, H., Li, X., Zhang, X., Kang, R., and Tang, D. (2016). CISD1 inhibits ferroptosis by protection against mitochondrial lipid peroxidation. Biochem. Biophys. Res. Commun. *478*, 838–844. https://doi.org/10.1016/j.bbrc.2016.08.034.
126. Huang, L.J., Zhan, S.T., Pan, Y.Q., Bao, W., and Yang, Y. (2023). The role of Vps4 in cancer development. Front. Oncol. *13*, 1203359. https://doi.org/10.3389/fonc.2023.1203359.
127. Galy, B., Conrad, M., and Muckenthaler, M. (2024). Mechanisms controlling cellular and systemic iron homeostasis. Nat. Rev. Mol. Cell Biol. *25*, 133–155. https://doi.org/10.1038/s41580-023-00648-1.
128. De Bock, M., Wang, N., Decrock, E., Bultynck, G., and Leybaert, L. (2015). Intracellular Cleavage of the Cx43 C-Terminal Domain by Matrix-Metalloproteases: A Novel Contributor to Inflammation? Mediators Inflamm. *2015*, 257471. https://doi.org/10.1155/2015/257471.
129. de Castro Bras, L.E., Cates, C.A., DeLeon-Pennell, K.Y., Ma, Y., Iyer, R.P., Halade, G.V., Yabluchanskiy, A., Fields, G.B., Weintraub, S.T., and Lindsey, M.L. (2014). Citrate synthase is a novel *in vivo* matrix metalloproteinase-9 substrate that regulates mitochondrial function in the postmyocardial infarction left ventricle. Antioxid. Redox Signaling *21*, 1974–1985. https://doi.org/10.1089/ars.2013.5411.
130. Kim, K., Punj, V., Kim, J.M., Lee, S., Ulmer, T.S., Lu, W., Rice, J.C., and An, W. (2016). MMP-9 facilitates selective proteolysis of the histone H3 tail at genes necessary for proficient osteoclastogenesis. Genes Dev. *30*, 208–219. https://doi.org/10.1101/gad.268714.115.
131. Vandenbroucke, R.E., and Libert, C. (2014). Is their new hope for therapeutic matrix metalloproteinase inhibition? Nat. Rev. Drug Discov. *13*, 904–927. https://doi.org/10.1038/nrd4390.
132. Augoff, K., Hryniewicz-Jankowska, A., Tabola, R., and Stach, K. (2022). MMP9: A Tough Target for Targeted Therapy for Cancer. Cancers *14*, 1847. https://doi.org/10.3390/cancers14071847.
133. Becirovic-Agic, M., Chalise, U., Daseke, M.J., 2nd, Konfrst, S., Salomon, J.D., Mishra, P.K., and Lindsey, M.L. (2021). Infarct in the Heart: What's MMP-9 Got to Do with It? Biomolecules *11*, 491. https://doi.org/10.3390/biom11040491.
134. Romanic, A.M., Harrison, S.M., Bao, W., Burns-Kurtis, C.L., Pickering, S., Gu, J., Grau, E., Mao, J., Sathe, G.M., Ohlstein, E.H., and Yue, T.L. (2002). Myocardial protection from ischemia/reperfusion injury by targeted deletion of matrix metalloproteinase-9. Cardiovasc. Res. *54*, 549–558. https://doi.org/10.1016/s0008-6363(02)00254-7.
135. Sundstrom, J., Evans, J.C., Benjamin, E.J., Levy, D., Larson, M.G., Sawyer, D.B., Siwik, D.A., Colucci, W.S., Sutherland, P., Wilson, P.W., and Vasan, R.S. (2004). Relations of plasma matrix metalloproteinase-9 to clinical cardiovascular risk factors and echocardiographic left ventricular measures: the Framingham Heart Study. Circulation *109*, 2850–2856. https://doi.org/10.1161/01.CIR.0000129318.79570.84.
136. Nandi, S.S., Zheng, H., Sharma, N.M., Shahshahan, H.R., Patel, K.P., and Mishra, P.K. (2016). Lack of miR-133a Decreases Contractility of Diabetic Hearts: A Role for Novel Cross Talk Between Tyrosine Aminotransferase and Tyrosine Hydroxylase. Diabetes *65*, 3075–3090. https://doi.org/10.2337/db16-0023.

## STAR★METHODS

### KEY RESOURCES TABLE

| REAGENT or RESOURCE | SOURCE | IDENTIFIER |
|---|---|---|
| Antibodies | | |
| MMP9 (N-terminal) Polyclonal antibody | Proteintech | Cat#10375-2-AP; RRID: AB_10897178 |
| Anti-Sp1 Antibody | Millipore | Cat#07-645; RRID: AB_310773 |
| CREB1 Polyclonal antibody | Proteintech | Cat#12208-1-AP; RRID: AB_2245417 |
| NRF2, NFE2L2 Polyclonal antibody | Proteintech | Cat#16396-1-AP; RRID: AB_2782956 |
| ATF4 Polyclonal antibody | Proteintech | Cat#10835-1-AP; RRID: AB_2058600 |
| FOXO3A Polyclonal antibody | Proteintech | Cat#10849-1-AP; RRID: AB_2247214 |
| Recombinant Anti-Glutathione Peroxidase 4 antibody | Abcam | Cat#ab125066; RRID: AB_10973901 |
| GSR Polyclonal antibody | Proteintech | Cat#18257-1-AP; RRID: AB_10598162 |
| GPX1 Polyclonal antibody | Proteintech | Cat#29329-1-AP; RRID: AB_2918283 |
| HO-1/HMOX1 Polyclonal antibody | Proteintech | Cat#10701-1-AP; RRID: AB_2118685 |
| Transferrin Receptor Monoclonal Antibody | ThermoFisher | Cat#13-6800; RRID: AB_86623 |
| Anti-Ferritin Light Chain antibody | Abcam | Cat#ab69090; RRID: AB_1523609 |
| PCBP1 Polyclonal Antibody | ThermoFisher | Cat#PA5-86055; RRID: AB_2802856 |
| SLC40A1/FPN1 Polyclonal antibody | Proteintech | Cat#26601-1-AP; RRID: AB_2880571 |
| MFN1 Polyclonal antibody | Proteintech | Cat#13798-1-AP; RRID: AB_2266318 |
| FTMT Polyclonal Antibody | ThermoFisher | Cat#PA5-30906; RRID: AB_2548380 |
| Anti-rabbit IgG, HRP-linked Antibody | Cell Signaling | Cat#7074; RRID: AB_2099233 |
| Anti-mouse IgG, HRP-linked Antibody | Cell Signaling | Cat#7076; RRID: AB_330924 |
| Malondialdehyde Monoclonal Antibody | ThermoFisher | Cat#MA5-27559; RRID: AB_2735264 |
| Chemicals, peptides, and recombinant proteins | | |
| Phorbol 12-myristate 13-acetate (PMA), PKC activator | Abcam | Cat#ab120297 |
| Critical commercial assays | | |
| Subcellular Protein Fractionation Kit for Cultured Cells | ThermoFisher | Cat#78840 |
| Cell Fractionation Kit | Abcam | Cat#ab109719 |
| GSH/GSSG Ratio Detection Assay Kit II (Fluorometric - Green) | Abcam | Cat#ab205811 |
| Cell Ferrous Iron Colorimetric Assay Kit | Elabscience | Cat#E-BC-K881-M |
| CyQUANT™ LDH Cytotoxicity Assay | ThermoFisher | Cat#C20300 |
| Duolink® *In Situ* PLA® Probe Anti-Rabbit MINUS | Millipore | Cat#DUO92005-100RXN |
| Duolink® *In Situ* PLA® Probe Anti-Mouse PLUS | Millipore | Cat#DUO92001-100RXN |
| Duolink® *In Situ* Red Starter Kit Mouse/Rabbit | Millipore | Cat#DUO92101-1KT |
| Experimental models: Cell lines | | |
| Human HEK293 cells | ATCC | Cat#CRL-1573 |
| Oligonucleotides | | |
| Plasmids | Vector Builder | https://www.vectorbuilder.com |

(*Continued on next page*)

*Continued*

| REAGENT or RESOURCE | SOURCE | IDENTIFIER |
|---|---|---|
| Software and algorithms | | |
| Fiji | Fiji | https://fiji.sc |
| ImageJ | National Institutes of Health (NIH) | https://imagej.nih.gov/ij/ |
| Zeiss Confocal Microscopy | Zeiss | https://www.zeiss.com/microscopy/int/home.html |
| GraphPad Prism 10 | GraphPad Software | https://www.graphpad.com/scientific-software/prism/ |
| IPA (Ingenuity Pathway Analysis) | QIAGEN | https://digitalinsights.qiagen.com/products-overview/discovery-insights-portfolio/analysis-and-visualization/qiagen-ipa/ |
| PyMOL | Schrödinger | https://pymol.org/2/ |
| ChimeraX | University of California, San Francisco (UCSF) | https://www.cgl.ucsf.edu/chimerax/ |
| AutoDock | Scripps Research | http://autodock.scripps.edu/ |
| ClusPro | Boston University | https://cluspro.org/ |
| PRODIGY | HADDOCK | https://nestor.science.uu.nl/prodigy/ |
| Cytoscape | Cytoscape Consortium | https://cytoscape.org/ |
| BioRender | BioRender | https://biorender.com/ |
| Image Lab | Bio-Rad | https://www.bio-rad.com/en-us/product/image-lab-software?ID=KRE6P5E8Z |
| Other | | |
| Mass Spectrometry Protein Identification | Creative Proteomics | https://www.creative-proteomics.com |

## RESOURCE AVAILABILITY

### Lead contact

Further information and request for resources and reagents should be directed to and will be fulfilled by the lead contact, Paras Kumar Mishra (paraskumar.mishra@unmc.edu).

### Materials availability

This study did not generate new unique reagents.

### Data and code availability

Data: All data reported will be shared by the lead contact upon request.

Code: This paper does not report original code.

Additional information required to analyze the data reported in this paper is available from the lead contact upon request.

## EXPERIMENTAL MODEL AND STUDY PARTICIPANT DETAILS

### Cell line

Human embryonic Kidney- 293 (HEK293) cells were procured from the American Type Culture Collection (ATCC) with number CRL-1573.

## METHOD DETAILS

### Cell culture

HEK293 cells were maintained in a complete growth medium consisting of Dulbecco's Modified Eagle Medium (DMEM) supplemented with 10% fetal bovine serum (FBS). Cells were used up to 10 passages and cell health was monitored daily. For transfection, cells were seeded in complete culture media and allowed to reach approximately 70-80% confluency. Transfection was performed using a polymer reagent (PolyJet) according to the manufacturer's instructions. Briefly, the polymer reagent and DNA constructs were mixed in Plain DMEM medium and incubated for a specified period to allow complex formation. The transfection mixture was then added dropwise to the cells and media was changed 5 h post transfection. Transfection efficiency was evaluated 24 h post transfection.

Following the transfection, the cells were treated with either PMA or an MMP9 inhibitor. PMA was added to a final concentration of 10 ng/mL and incubated for 24 h. The MMP9 inhibitor, at a concentration of 5 μM, was added to the cells 5 h post transfection. Both PMA and the MMP9 inhibitor were prepared as stock solutions in suitable solvents and diluted in the growth medium to achieve the desired concentrations.

After the treatment, the cells were further incubated for 24 h to allow the desired cellular response. The experimental conditions were replicated in independent wells to ensure reliable results. Subsequently, the cells were harvested in RIPA buffer with protease and phosphatase inhibitor cocktail for downstream analysis, except for zymography.

### Cell fractionation

In our study, cellular fractionation was carried out using the Abcam Cell Fractionation Kit - Standard (ab109719), following the manufacturer's provided protocol. Briefly, cells were harvested and subjected to a series of differential centrifugations and extractions, as prescribed by the kit instructions. This process involved the use of a proprietary buffer system to ensure the selective and sequential extraction of proteins from different cellular compartments. The integrity and purity of each fraction were assessed by Western blotting, using marker proteins specific to each cellular compartment and another marker that is not specific to the fractionation to assess the fraction purity.

### Cytotoxicity assay

For assessing cell cytotoxicity, we employed the CyQUANT™ LDH Cytotoxicity Assay (Thermo Fisher Scientific, C20300), in accordance with the manufacturer's instructions. This assay is designed to measure lactate dehydrogenase (LDH) activity released into the culture medium from damaged cells, serving as an indicator of cellular membrane integrity and cytotoxicity. Briefly, after transfection and treatment with lysis buffer (Maximum LDH control), supernatants were transferred to a different 96-well plates. The plates were then incubated 37°C for 45 minutes, protected from light, to allow the development of the colorimetric reaction. The optical density was measured at 490 and 680 nm using a microplate reader. The percentage of cytotoxicity was calculated by comparing the LDH release from treated cells to that from maximum LDH release controls, which were lysed with the provided lysis solution, enabling us to quantify the cytotoxic effects of the compounds on the cells, following the manufacturer's instructions.

### Western blotting

Western blotting was performed following a previously established lab protocol.[136] Briefly, HEK293 cells were lysed using RIPA lysis buffer containing protease inhibitors and protein concentration was determined by BCA assay. Proteins were loaded in SDS-PAGE gel and transferred to nitrocellulose membrane using a wet transfer system. The membrane was then blocked with a 5% non-fat milk and incubated with primary antibody (1:1000 dilution) overnight at 4°C. The membrane was washed and then incubated with secondary antibody conjugated to horseradish peroxidase (1:2000 dilution) at room temperature for 2 h. After washing, protein bands were observed under a Bio-Rad ChemiDoc imaging system. The protein bands were quantified using the Image Lab analysis software, and total Protein was used for normalization.

### Co-immunoprecipitation

For Co-immunoprecipitation (co-IP), 2 mg of protein was incubated with magnetic Dynabeads (Thermo Fisher Scientific) following the manufacturer's instructions. An additional 25 g of total protein was loaded onto a separate gel and stained with Coomassie blue for normalization. BioRad ChemiDoc instrument and its software was used to capture the image and analyze the bands. Experiments using co-IP were conducted with positive and negative controls in triplicate.

### Proximal ligation assay (PLA)

Millipore Sigma's Duolink® *In Situ* Red Starter Kit Mouse/Rabbit was used for the Proximal Ligation Assay. We cultured 5 X 10^5 cells in 50 μl medium in a μ-Slide 15-well-3D glass bottom, which was purchased from Ibidi. After fixing the cells for 15 minutes at the room temperature with 4% paraformaldehyde, they were rinsed three times with phosphate buffered Saline (PBS). The cells were then stained with 5g/ml Wheat Germ Agglutinin (WGA) in PBS and incubated for 5 minutes at room temperature in the dark. To permeabilize the cells, they were subjected to 50 μl of ice-cold 100 percent methanol for 30 minutes at -20°C, followed by three washing in PBS. The PLA was performed following manufacturer's instructions. Images were captured using a Zeiss 710 Confocal Laser Scanning microscope equipped with a 63x oil lens and available at the University of Nebraska Medical Center core facilities.

### In-silico protein-protein interaction

We obtained the protein structures from the RCSB PDB. To examine protein-protein or protein-ligand interactions, molecular docking was done using a combination of the ClusPro 2.0 website and the AutoDock program. Using UCSF ChimeraX and Pymol programs, the protein models were subjected to intensive analysis, allowing for a thorough evaluation of the docking conformations and probable binding locations. To measure protein binding affinity, Prodigy webserver was used in the analysis.

### Ingenuity pathway analysis (IPA)

To predict MMP9's activity in the ferroptosis pathway using IPA Qiagen software, we employed the molecular activity predictor (MAP) feature, focusing on analyzing its activation and inhibition impact on the ferroptosis pathway. This step provided insights into MMP9's activation and inhibition state and its effects on downstream molecules, enabling a targeted analysis of its role within the pathway.

### Confocal microscopy

In our investigation of protein-protein interactions via Proximity Ligation Assays (PLA), confocal microscopy imaging was performed at the University of Nebraska Medical Center (UNMC) Core Facility. Following the PLA protocol using Duolink® PLA probes (Sigma-Aldrich) on prepared cell samples, imaging was conducted using a high-resolution confocal microscope equipped with a 63x zoom lens. This setup allowed for precise visualization of the interactions at a molecular level, with the advanced imaging software of the facility used to finely tune parameters for optimal signal clarity and minimal background interference.

### MMP9 and mutant MMP9 expression vectors

The plasmid was synthesized using Vector builder services. The coding sequence for MMP9 and the mutant collagenase site of MMP9 proteins were inserted downstream of the CMV promoter, which was selected to achieve optimal expression in the target host system. To facilitate protein detection and localization studies, we incorporated the coding sequence for the EGFR/RFP fusion protein into both plasmids. To prevent any potential disruption to the structure and function of MMP9 protein, we selected a separate promoter for the EGFR/RFP protein that would not interfere with the expression or folding of MMP9.

### Liquid chromatography with tandem mass spectrometry (LC-MS/MS) analysis

In this study, protein identification was performed following the protocol provided by Creative Proteomics. Initially, 1 mg of proteins were used for co-immunoprecipitation (co-IP). Post co-IP, samples underwent SDS-PAGE and subsequent in-gel digestion with trypsin. The digested proteins were then identified using a nano LC-MS/MS platform.

The key reagents, including DL-dithiothreitol (DTT), iodoacetamide (IAA), formic acid (FA), and acetonitrile (ACN), were sourced from Sigma and Promega, with ultrapure water prepared using a Millipore system. The mass spectrometry analysis was conducted on a Q Exactive HF mass spectrometer (Thermo Fisher Scientific, USA) coupled with an Ultimate 3000 nano UHPLC system.

The SDS-PAGE process involved running the gel at specified voltages and staining with silver. The in-gel digestion comprised multiple steps, including washing, dehydration, reduction, and alkylation of the gel slices, followed by overnight trypsin digestion. The peptides were extracted, lyophilized, and resuspended in 0.1% formic acid for LC-MS/MS analysis.

Nano LC utilized a trapping and analytical column from PepMap C18, with a detailed LC gradient and flow rate. The mass spectrometry settings included a full scan range of 300-1,650 m/z and a Top 20 MS/MS scan with specific resolution, gain control, injection time, and collision energy parameters.

Finally, data analysis was performed using Maxquant software against a human protein database, with specific parameters for protein modifications, enzyme specificity, cleavage, and ion mass tolerance. The comprehensive protein and peptide identification details were recorded in supplemental excel sheets (Table S1).

## QUANTIFICATION AND STATISTICAL ANALYSIS

Data are presented as the mean ± standard error of the mean (SEM). To assess the statistical differences between groups, we employed either one-way or two-way analysis of variance (ANOVA), complemented by post-hoc tests for detailed comparisons. A P-value of less than 0.05 was considered statistically significant (* indicates $P < 0.05$, ** indicates $P < 0.01$, *** indicates $P < 0.001$, and **** indicates $P < 0.0001$). All statistical analyses were conducted using Prism 10.0 software. Details of each experiment and statistical analysis are included in the Figure Legends.